Elastic Shape Registration of Surfaces in 3D Space with Gradient Descent and Dynamic Programming

Javier Bernal[1], Jim Lawrence[1,2]

[1]*National Institute of Standards and Technology,*

Gaithersburg, MD 20899, USA

[2]*George Mason University,*

4400 University Dr, Fairfax, VA 22030, USA

{javier.bernal,james.lawrence}

@nist.gov lawrence@gmu.edu

Abstract

Algorithms based on gradient descent for computing the elastic shape registration of two simple surfaces in 3−dimensional space and therefore the elastic shape distance between them have been proposed by Kurtek, Jermyn, et al., and more recently by Riseth. Their algorithms are designed to minimize a distance function between the surfaces by rotating and reparametrizing one of the surfaces, the minimization for reparametrizing based on a gradient descent approach that may terminate at a local solution. On the other hand, Bernal and Lawrence have proposed a similar algorithm, the minimization for reparametrizing based on dynamic programming thus producing a partial not necessarily optimal elastic shape registration of the surfaces. Accordingly, Bernal and Lawrence have proposed to use the rotation and reparametrization computed with their algorithm as the initial solution to any algorithm based on a gradient descent approach for reparametrizing. Here we present results from doing exactly that. We also describe and justify the gradient descent approach that is used for reparametrizing one of the surfaces.

MSC: 15A15, 15A18, 65D07, 65K99, 90C39

Keywords: dynamic programming, elastic shape distance, diffeomorphism, gradient descent, reparametrization, shape analysis

1 Introduction

In this paper, we present results from computing the elastic shape registration of two simple surfaces in 3−dimensional space and the elastic shape distance between them with an algorithm based on a gradient descent approach for reparametrizing one of the surfaces similar to those in [6, 10], and more recently in [12], using as the input initial solution to the algorithm the rotation and reparametrization computed with the algorithm based on dynamic programming presented in [3] for reparametrizing one of the surfaces to obtain a partial elastic shape registration of the surfaces. We note, the gradient descent approach used to obtain our results is a generalization to surfaces in 3−dimensional space of the gradient descent approach for reparametrizing one of two curves in the plane when computing the elastic shape distance between them as presented in [13]. For the sake of completeness, we describe and justify the approach for curves as it is done there, and then present and justify its generalization to surfaces in 3−dimensional space. This generalization together with its justification was developed independently of similar work in [6, 10, 12].

Given that S_1 and S_2 are the two surfaces under consideration, we assume they are *simple*, that is, we assume that for $D = [0,1] \times [0,1]$ in the xy plane ($\mathbb{R}^2$), i.e., the unit square in the plane, one-to-one functions c_1 and c_2 of class C^1 exist, $c_1 : D \to \mathbb{R}^3$, $c_2 : D \to \mathbb{R}^3$, such that $S_1 = c_1(D)$ and $S_2 = c_2(D)$. We then say that c_1 and c_2 *parametrize* or are *parametrizations* of S_1 and S_2, respectively, and that S_1 and S_2 are *parametrized surfaces* relative to c_1 and c_2, respectively. In addition, given a surface S in 3−dimensional space and one-to-one functions c, p of class C^1, $c : D \to \mathbb{R}^3$, $p : D \to \mathbb{R}^3$, $c(D) = S$, $p(D) = S$, so that c and p are parametrizations of S, we say p is a *reparametrization* of c or that p *reparametrizes* S (given as an image of c), if $p = c \circ h$ for a diffeomorphism h from D onto D.

The computation of the elastic shape registration of two surfaces in 3D space together with the elastic shape distance between them has applications in the study of geological terrains, surfaces of anatomical objects and structures such as facial surfaces, etc. Figure 1 shows the boundaries (solid blue and dashed red) of two surfaces of sinusoidal shape. Their shapes are identical so that the elastic shape distance between them is zero. Note, the $x-$,

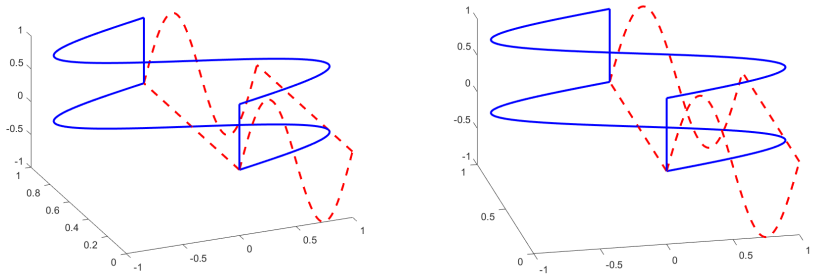


Figure 1: Views of the boundaries of two surfaces in 3D space of identical sinusoidal shapes so that the elastic shape distance between them is zero.

$y-$ and $z-$ axes in the figure are not to scale relative to one another.

2 The Shape Function of a Parametrized Surface

In this section we recall the definition of the shape function of a parametrized surface in 3-dimensional space as introduced in [3]. A similar definition has been presented in [1, 2, 7, 13, 14] in the context of the shape function of a parametrized curve in $d-$dimensional space, d any positive integer. Accordingly, in [1, 2, 7, 13, 14], given $\beta : [0,1] \to \mathbb{R}^d$ of class C^1, a parametrization of a curve in $\mathbb{R}^d$, the shape function q of β, i.e., the shape function q of the curve that β parametrizes, $q : [0,1] \to \mathbb{R}^d$, is defined by $q(t) = \dot{\beta}(t)/\sqrt{||\dot{\beta}(t)||}$, $t \in [0,1]$ ($d-$dimensional 0 if $\dot{\beta}(t)$ equals $d-$dimensional 0). It follows then that q is square integrable as

$$\int_0^1 ||q(t)||^2 dt = \int_0^1 ||\dot{\beta}(t)/\sqrt{||\dot{\beta}(t)||}\,||^2 dt = \int_0^1 ||\dot{\beta}(t)|| dt$$

which is the length of the curve that β parametrizes, where $||\cdot||$ is the $d-$dimensional Euclidean norm. Again with q the shape function of β and Γ the set of orientation-preserving diffeomorphisms of $[0,1]$ so that for $\gamma \in \Gamma$ then $\dot{\gamma} \geq 0$ on $[0,1]$, it then follows that for $\gamma \in \Gamma$ the shape function of the reparametrization $\beta \circ \gamma$ of β is $(q,\gamma) = (q \circ \gamma)\sqrt{\dot{\gamma}}$. With $||q||_2 = (\int_0^1 ||q(t)||^2 dt)^{1/2}$, we also note that given β_1, $\beta_2 : [0,1] \to \mathbb{R}^d$ of class C^1, parametrizations of curves in $\mathbb{R}^d$ with shape functions q_1, q_2, respectively, then $||(q_1,\gamma) - (q_2,\gamma)||_2 = ||q_1 - q_2||_2$ for any $\gamma \in \Gamma$, and from this, etc., with

$\Gamma_0 = \{\gamma \in \Gamma,\ \dot{\gamma} > 0 \text{ on } [0,1]\}$, $SO(d)$ the set of $d \times d$ rotation matrices, it has been demonstrated [1, 4, 13] that the number $\inf_{R \in SO(d), \gamma \in \Gamma_0} ||Rq_1 - (q_2, \gamma)||_2$ can then be used as a well-defined distance between the two curves that β_1, β_2 parametrize, β_1 and β_2 both normalized to parametrize curves of length 1.

As for the definition of the shape function of a parametrized surface in 3-dimensional space, again with $D = [0,1] \times [0,1]$ in the xy plane ($\mathbb{R}^2$), given a one-to-one function c of class C^1, $c : D \to \mathbb{R}^3$, so that for (u, v) in D, c takes (u, v) to $c(u, v)$ in $\mathbb{R}^3$, c a parametrization of a surface S in 3−dimensional space, the shape function q of c, $q : D \to \mathbb{R}^3$, i.e., the shape function q of the surface S that c parametrizes is defined by

$$q(u,v) = (\frac{\partial c}{\partial u}(u,v) \times \frac{\partial c}{\partial v}(u,v)) / \sqrt{||\frac{\partial c}{\partial u}(u,v) \times \frac{\partial c}{\partial v}(u,v)||}$$

(3−dimensional 0 if $\frac{\partial c}{\partial u}(u,v) \times \frac{\partial c}{\partial v}(u,v)$ equals 3−dimensional 0), where $||\cdot||$ is the 3−dimensional Euclidean norm. It follows then that q is square integrable as

$$\int \int_D ||q(u,v)||^2 du\, dv = \int \int_D ||\frac{\partial c}{\partial u}(u,v) \times \frac{\partial c}{\partial v}(u,v)||\, du\, dv$$

which is the surface area of S.

With c, q, D, S as above, in a manner similar to the one described above in the context of the shape function of the parametrization of a curve in d−dimensional space, the shape function of a reparametrization of c can be computed from the shape function q of c. With p as a reparametrization of c, i.e., p a parametrization of S and $p = c \circ h$ for a diffeomorphism h from D onto D, $h(r,t) = (h_1(r,t), h_2(r,t))$, assuming $\frac{\partial h}{\partial (r,t)} \geq 0$ on D, $\frac{\partial h}{\partial (r,t)}$ the determinant of the Jacobian of h, i.e., $\frac{\partial h}{\partial (r,t)} = \frac{\partial h_1}{\partial r}\frac{\partial h_2}{\partial t} - \frac{\partial h_1}{\partial t}\frac{\partial h_2}{\partial r}$, and defining a function on D into $\mathbb{R}^3$, which we denote by (q, h),

$$(q,h) \equiv (q \circ h)\sqrt{\frac{\partial h}{\partial (r,t)}},$$

then as established in [3] the shape function on D of the reparametrization $p = c \circ h$ of c is then (q, h).

We note as well, given D, h, $\frac{\partial h}{\partial(r,t)}$ as above, $\frac{\partial h}{\partial(r,t)} \geq 0$ on D; S_1, S_2 surfaces, c_1, c_2 parametrizations of S_1, S_2, respectively, p_1, p_2 parametrizations of S_1, S_2, respectively, p_1, p_2 reparametrizations of c_1, c_2, respectively, $p_1 = c_1 \circ h$, $p_2 = c_2 \circ h$; q_1, q_2, $\hat{q}_1$, $\hat{q}_2$ the shape functions of c_1, c_2, p_1, p_2, respectively, then as established in [3], with $h(r,t) = (h_1(r,t), h_2(r,t)) = (u(r,t), v(r,t))$,

$$\begin{aligned} ||\hat{q}_1 - \hat{q}_2||_2 &\equiv \Big(\int\int_D ||\hat{q}_1 - \hat{q}_2)||^2 dr\, dt\Big)^{1/2} \\ &= \Big(\int\int_D ||q_1 - q_2||^2 du\, dv\Big)^{1/2} \\ &\equiv ||q_1 - q_2||_2. \end{aligned}$$

Based on results about shape functions of parametrized surfaces such as the results above, and using arguments similar to arguments for justifying the definition of the distance between curves in $d-$dimensional space found in [1, 4, 13], it has been demonstrated as pointed out in [3] that with D as above, given two simple surfaces S_1 and S_2 parametrized by functions c_1 and c_2, $c_1 : D \to \mathbb{R}^3$, $c_2 : D \to \mathbb{R}^3$, $S_1 = c_1(D)$, $S_2 = c_2(D)$, letting $SO(3)$ be the set of 3×3 rotation matrices, Σ_0 the set of all diffeomorphisms h from D onto D, with $h(r,t) = (h_1(r,t), h_2(r,t))$, $\frac{\partial h}{\partial(r,t)} > 0$ on D, $\frac{\partial h}{\partial(r,t)}$ the determinant of the Jacobian of h, and q_1 and q_2 the shape functions of c_1 and c_2, respectively, the number $\inf_{R \in SO(3), h \in \Sigma_0} ||Rq_1 - (q_2, h)||_2$, i.e.,

$$\inf_{R \in SO(3), h \in \Sigma_0} \Big(\int\int_D ||Rq_1 - (q_2, h)||^2 dr\, dt\Big)^{1/2} =$$

$$\inf_{R \in SO(3), h \in \Sigma_0} \Big(\int_0^1 \int_0^1 \Big|\Big|Rq_1 - (q_2 \circ h)\sqrt{\frac{\partial h}{\partial(r,t)}}\Big|\Big|^2 dr\, dt\Big)^{1/2}$$

can be used as a well-defined distance between the surfaces S_1 and S_2, c_1 and c_2 both normalized to parametrize surfaces of area equal to 1.

3 Gradient Descent Optimization over the Group of Reparametrizations of a Curve in the Plane

In this section, for the sake of completeness, we describe and justify the gradient descent approach in [13] in the same way it is done there, for

reparametrizing one of two curves in the plane when computing the elastic shape distance between them. In what follows, Γ_I will denote the set of functions $\gamma : [0,1] \to [0,1]$, with $\gamma(0) = 0$, $\gamma(1) = 1$, such that γ^{-1}, the inverse of γ, exists, both γ and γ^{-1} are smooth, and $\dot{\gamma} > 0$ on $[0,1]$. With $H : \Gamma_I \to \mathbb{R}_{\geq 0}$ defined by

$$H(\gamma) = \int_0^1 ||q_1(t) - q_2(\gamma(t))\sqrt{\dot{\gamma}(t)}||^2 \, dt,$$

where q_1, q_2 are shape functions of parametrized curves in the plane of length 1, the goal then is to find $\gamma \in \Gamma_I$ that minimizes $H(\gamma)$.

In order to find any such γ with a gradient approach, as illustrated below, a gradient of H is computed with respect to Γ_I at the k^{th} iteration of the approach, from which γ_k and $\gamma^{(k)}$ in Γ_I are then computed, so that inductively with γ_0 in Γ_I as an initial solution, γ_0 possibly equal to the identity function γ_{id} in Γ_I, then $\gamma^{(k)} = \gamma_0 \circ \gamma_1 \circ \ldots \circ \gamma_k$, and $H(\gamma^{(0)}) > H(\gamma^{(1)}) > \ldots > H(\gamma^{(k)})$. In reality, inductively, with $\tilde{q}_2 = (q_2 \circ \gamma^{(k-1)})\sqrt{\dot{\gamma^{(k-1)}}}$, at the k^{th} iteration of the approach it is the gradient of

$$H_k(\gamma) = \int_0^1 ||q_1(t) - \tilde{q}_2(\gamma(t))\sqrt{\dot{\gamma}(t)}||^2 \, dt$$

that is actually computed, from which γ_k is computed, and as verified below, with $\gamma^{(k)}$ as above, then $H(\gamma^{(k)}) = H_k(\gamma_k)$.

With $[q_2]_{\Gamma_I}$ denoting the orbit of q_2, i.e., $[q_2]_{\Gamma_I} = \{\tilde{q} \mid \tilde{q} = (q_2 \circ \gamma)\sqrt{\dot{\gamma}},\ \gamma \in \Gamma_I\}$, and $\tilde{q}_2$ in $[q_2]_{\Gamma_I}$ given by $\tilde{q}_2 = (q_2 \circ \gamma^{(k)})\sqrt{\dot{\gamma^{(k)}}}$, at the $(k+1)^{th}$ iteration of the approach, letting $T_{\tilde{q}_2}([q_2]_{\Gamma_I})$ be the tangent space to $[q_2]_{\Gamma_I}$ at $\tilde{q}_2$, $T_{\gamma_{id}}(\Gamma_I)$ the tangent space to Γ_I at γ_{id}, and ϕ the mapping from Γ_I into $[q_2]_{\Gamma_I}$ defined by $\phi(\gamma) = (\tilde{q}_2 \circ \gamma)\sqrt{\dot{\gamma}}$, $\gamma \in \Gamma_I$, since $\phi(\gamma_{id}) = \tilde{q}_2$, then the differential $d\phi_{\gamma_{id}} : T_{\gamma_{id}}(\Gamma_I) \to T_{\tilde{q}_2}([q_2]_{\Gamma_I})$ of ϕ at γ_{id} can be defined. Accordingly, given v in $T_{\gamma_{id}}(\Gamma_I)$, the lemma that follows shows how to compute $d\phi_{\gamma_{id}}(v)$, and using the result of this computation, the theorem that also follows shows how to compute at the $(k+1)^{th}$ iteration of the approach the directional derivative $\nabla_v H$ of H (actually $\nabla_v H_{k+1}$ of H_{k+1}) in the direction of v.

We note then that given v_i, $i = 1, 2, 3, \ldots$, an orthonormal basis of the vector

space $T_{\gamma_{id}}(\Gamma_I)$ under some metric, e.g., $\frac{1}{\sqrt{2}\pi n}\sin(2\pi nt)$, $\frac{1}{\sqrt{2}\pi n}(\cos(2\pi nt)-1)$, $t\in[0,1]$, $n=1,2,3,\ldots$, under the Palais metric, $\sqrt{2}\sin(m\pi t)$, $t\in[0,1]$, $m=1,2,3,\ldots$, under the L^2 metric, at the $(k+1)^{th}$ iteration of the approach the gradient of H_{k+1} is approximated by $\nabla H_{k+1}=\sum_{i=1}^{N}(\nabla_{v_i}H_{k+1})v_i$, for a large N. If under the same metric ∇H_{k+1} is considered to be small enough, then $\gamma^{(k)}$ is taken to be the solution of the gradient descent approach, although perhaps a local solution. Otherwise, using a small step size $\delta>0$, γ_{k+1} and $\gamma^{(k+1)}$ are computed, $\gamma_{k+1}=\gamma_{id}-\delta\ \nabla H_{k+1}$, $\gamma^{(k+1)}=\gamma^{(k)}\circ\gamma_{k+1}$. That $\gamma^{(k+1)}$ is computed so that $H(\gamma^{(k+1)})=H_{k+1}(\gamma_{k+1})$ follows by letting $\tilde{q}_2$ be as obtained at the k^{th} iteration of the approach, and proving that

$$(q_2\circ\gamma^{(k+1)})\sqrt{\dot{\gamma^{(k+1)}}}=(\tilde{q}_2\circ\gamma_{k+1})\sqrt{\dot{\gamma_{k+1}}}\ \text{ as is done here:}$$

$$\begin{aligned}
&(\tilde{q}_2\circ\gamma_{k+1})\sqrt{\dot{\gamma_{k+1}}}=((q_2\circ\gamma^{(k)})\sqrt{\dot{\gamma^{(k)}}})\circ\gamma_{k+1})\sqrt{\dot{\gamma_{k+1}}}\\
=\ &(q_2\circ\gamma^{(k)}\circ\gamma_{k+1})\sqrt{\dot{\gamma^{(k)}}\circ\gamma_{k+1}}\sqrt{\dot{\gamma_{k+1}}}\\
=\ &(q_2\circ\gamma^{(k)}\circ\gamma_{k+1})\sqrt{(\dot{\gamma^{(k)}}\circ\gamma_{k+1})\dot{\gamma_{k+1}}}=(q_2\circ\gamma^{(k+1)})\sqrt{\dot{\gamma^{(k+1)}}}.
\end{aligned}$$

The lemma and theorem follow. Here shape functions are C^1 as well.

Lemma 1: Given q, the shape function of a curve in the plane, $\phi:\Gamma_I\to[q]_{\Gamma_I}$, $\phi(\gamma)=(q\circ\gamma)\sqrt{\dot{\gamma}}$, then given γ in Γ_I, v in $T_\gamma(\Gamma_I)$, with $\dot{q}$ the Jacobian of q, the differential of ϕ at γ applied on v is

$$(d\phi_\gamma(v))(s)=\sqrt{\dot{\gamma}(s)}\dot{q}(\gamma(s))v(s)+\frac{1}{2\sqrt{\dot{\gamma}(s)}}\dot{v}(s)q(\gamma(s)),\ s\in[0,1].$$

Proof: Let $\alpha(\tau,\cdot)$ be a differentiable path in Γ_I passing through γ at $\tau=0$, i.e., $\alpha(0,s)=\gamma(s)$, $s\in[0,1]$. Let the velocity of this path at $\tau=0$ be given by $v\in T_\gamma(\Gamma_I)$, i.e., $v(s)=\frac{\partial\alpha}{\partial\tau}(0,s)$, $s\in[0,1]$. Note as well that $\frac{\partial\alpha}{\partial s}(0,s)=\dot{\gamma}(s)$, $\frac{\partial^2\alpha}{\partial s\partial\tau}(0,s)=\dot{v}(s)$, $s\in[0,1]$.

Since $\alpha(\tau,\cdot)$ is a path in Γ_I, then $\phi(\alpha(\tau,\cdot))$ is the corresponding path in $[q]_{\Gamma_I}$, and since v is the velocity of $\alpha(\tau,\cdot)$ at $\tau=0$, then the velocity of $\phi(\alpha(\tau,\cdot))$

at $\tau = 0$ is $d\phi_\gamma(v)$, that is to say

$$\begin{aligned}(d\phi_\gamma(v))(s) &= \frac{\partial}{\partial\tau}|_{\tau=0}\ \phi(\alpha(\tau,s)) = \frac{\partial}{\partial\tau}|_{\tau=0}\ \Big(\sqrt{\frac{\partial\alpha}{\partial s}(\tau,s)}\ q(\alpha(\tau,s))\Big)\\ &= \Big(\sqrt{\frac{\partial\alpha}{\partial s}(\tau,s)}\ \dot{q}(\alpha(\tau,s))\ \frac{\partial\alpha}{\partial\tau}(\tau,s) + \\ &\quad \frac{1}{2\sqrt{\frac{\partial\alpha}{\partial s}(\tau,s)}}\ \frac{\partial^2\alpha}{\partial\tau\partial s}(\tau,s)\ q(\alpha(\tau,s))\Big)|_{\tau=0}\\ &= \sqrt{\dot{\gamma}(s)}\dot{q}(\gamma(s))v(s) + \frac{1}{2\sqrt{\dot{\gamma}(s)}}\dot{v}(s)q(\gamma(s)),\ s\in[0,1].\end{aligned}$$

□

Corollary 1: Given q, ϕ, v as above, then

$$(d\phi_{\gamma_{id}}(v))(s) = \dot{q}(s)v(s) + \frac{1}{2}\dot{v}(s)q(s),\ s\in[0,1].$$

Theorem 1: With $H_{k+1}(\gamma) = \int_0^1 ||q_1(t) - \tilde{q}_2(\gamma(t))\sqrt{\dot{\gamma}(t)}||^2 dt$ so that $\tilde{q}_2 = (q_2\circ\gamma^{(k)})\sqrt{\dot{\gamma^{(k)}}}$ from the definition of H_{k+1}, then the directional derivative of H_{k+1} in the direction of $v\in T_{\gamma_{id}}(\Gamma_I)$ is

$$\nabla_v H_{k+1} = -2\int_0^1 \Big\langle q_1(t) - \tilde{q}_2(t)\ ,\ \dot{\tilde{q}}_2(t)v(t) + \frac{1}{2}\tilde{q}_2(t)\dot{v}(t)\Big\rangle dt.$$

Proof: Let $\alpha(\tau,\cdot)$ be a differentiable path in Γ_I passing through γ_{id} at $\tau = 0$, i.e., $\alpha(0,t) = \gamma_{id}(t)$, $t\in[0,1]$, with the velocity of this path at $\tau = 0$ equal to v, i.e., $\frac{\partial\alpha}{\partial\tau}(0,t) = v(t)$, $t\in[0,1]$.

Note, $H_{k+1}(\alpha(\tau,t))$ equals

$$\int_0^1 \Big\langle q_1(t) - \tilde{q}_2(\alpha(\tau,t))\sqrt{\frac{\partial\alpha}{\partial t}(\tau,t)}\ ,\ q_1(t) - \tilde{q}_2(\alpha(\tau,t))\sqrt{\frac{\partial\alpha}{\partial t}(\tau,t)}\Big\rangle dt.$$

Using the fact that in general $\frac{d}{ds}\langle f(s),g(s)\rangle = \langle f(s),g'(s)\rangle + \langle f'(s),g(s)\rangle$, from which $\frac{d}{ds}\langle f(s),f(s)\rangle = 2\langle f(s),f'(s)\rangle$, then differentiating $H_{k+1}(\alpha(\tau,t))$ with respect to τ by differentiating this last integral with respect to τ (done under the integral), and setting τ equal to zero, gives $\nabla_v H_{k+1}$ equals

$$2\int_0^1 \Big\langle q_1(t) - \tilde{q}_2(\gamma_{id}(t))\sqrt{\dot{\gamma}_{id}(t)}\ ,\ \frac{\partial}{\partial\tau}|_{\tau=0}\Big(-\tilde{q}_2(\alpha(\tau,t))\sqrt{\frac{\partial\alpha}{\partial t}(\tau,t)}\Big)\Big\rangle dt$$

$$= -2\int_0^1 \Big\langle q_1(t) - \tilde{q}_2(t)\ ,\ \frac{\partial}{\partial\tau}|_{\tau=0}\Big(\tilde{q}_2(\alpha(\tau,t))\sqrt{\frac{\partial\alpha}{\partial t}(\tau,t)}\Big)\Big\rangle dt$$

$$= -2\int_0^1 \Big\langle q_1(t) - \tilde{q}_2(t)\ ,\ \dot{\tilde{q}}_2(t)v(t) + \frac{1}{2}\tilde{q}_2(t)\dot{v}(t)\Big\rangle dt$$

by Corollary 1 and the proof of Lemma 1 as α here is the same as α there with γ equal to γ_{id}. □

Note that given $\gamma \in \Gamma_I$ and a differentiable path $\alpha(\tau,\cdot)$ in Γ_I through γ at $\tau = 0$, i.e., $\alpha(0,t) = \gamma(t)$, $t \in [0,1]$, then since for any real numbers τ_1, τ_2, close or equal to 0, $\alpha(\tau_1,0) - \alpha(\tau_2,0) = 0 - 0 = 0$ and $\alpha(\tau_1,1) - \alpha(\tau_2,1) = 1 - 1 = 0$, it can also be shown that

$$T_\gamma(\Gamma_I) = \{v : [0,1] \to \mathbb{R} \mid v(0) = 0, v(1) = 0,\ v \text{ smooth}\}.$$

We note that under this identification of $T_\gamma(\Gamma_I)$, each member of either of the sets of functions given above as examples of bases for $T_{\gamma_{id}}(\Gamma_I)$ is indeed in $T_{\gamma_{id}}(\Gamma_I)$.

4 Gradient Descent Optimization over the Group of Reparametrizations of a Surface in 3D Space

In this section, inspired by ideas used in the previous section, we describe and justify a gradient descent approach for reparametrizing one of two surfaces in 3−dimensional space when computing the elastic shape distance between them. The approach is a generalization to surfaces in 3−dimensional space of the gradient descent approach for reparametrizing one of two curves in the plane when computing the elastic shape distance between them as presented in [13] and in the previous section. This generalization together with its justification was developed independently of similar work in [6, 10, 12]. Again with D the unit square in the plane, in what follows, Γ_D will denote the set of functions $h : D \to D$, with $h(r,t) = (h_1(r,t), h_2(r,t))$, $(r,t) \in D$, satisfying boundary conditions $h_1(0,t) = 0$, $h_2(r,0) = 0$, $h_1(1,t) = 1$, $h_2(r,1) = 1$, such that h^{-1}, the inverse of h, exists, both h and h^{-1} are smooth, and $\frac{\partial h}{\partial(r,t)} > 0$ on D, $\frac{\partial h}{\partial(r,t)}$ the determinant of the Jacobian of h, i.e., $\frac{\partial h}{\partial(r,t)} = \frac{\partial h_1}{\partial r}\frac{\partial h_2}{\partial t} - \frac{\partial h_1}{\partial t}\frac{\partial h_2}{\partial r}$.

With $H : \Gamma_D \to \mathbb{R}_{\geq 0}$ defined by

$$H(h) = \int_0^1 \int_0^1 \Big|\Big| q_1(r,t) - q_2(h(r,t)) \sqrt{\frac{\partial h}{\partial (r,t)}(r,t)} \Big|\Big|^2 dr\, dt,$$

where q_1, q_2 are shape functions of parametrized surfaces in $3-$dimensional space of surface area 1, the goal then is to find $h \in \Gamma_D$ that minimizes $H(h)$.

Again, inspired by ideas used in the previous section, in order to find any such $h \in \Gamma_D$ with a gradient approach, as illustrated below, a gradient of H is computed with respect to Γ_D at the k^{th} iteration of the approach, from which h_k and $h^{(k)}$ in Γ_D are then computed, so that inductively with h_0 in Γ_D as an initial solution, h_0 possibly equal to the identity function h_{id} in Γ_D, or possibly equal to another element of Γ_D such as one computed with the algorithm based on dynamic programming presented in [3] that partially minimizes $H(h)$, then $h^{(k)} = h_0 \circ h_1 \circ \ldots \circ h_k$, and $H(h^{(0)}) > H(h^{(1)}) > \ldots > H(h^{(k)})$. In reality, inductively, with $\tilde{q}_2(r,t) = q_2(h^{(k-1)}(r,t)) \sqrt{\frac{\partial h^{(k-1)}}{\partial (r,t)}(r,t)}$, $(r,t) \in D$, at the k^{th} iteration of the approach it is the gradient of

$$H_k(h) = \int_0^1 \int_0^1 \Big|\Big| q_1(r,t) - \tilde{q}_2(h(r,t)) \sqrt{\frac{\partial h}{\partial (r,t)}(r,t)} \Big|\Big|^2 dr\, dt$$

that is actually computed, from which h_k is computed, and as verified below, with $h^{(k)}$ as above, then $H(h^{(k)}) = H_k(h_k)$.

With $[q_2]_{\Gamma_D}$ denoting the orbit of q_2, i.e.,

$$[q_2]_{\Gamma_D} = \Big\{ \tilde{q} \mid \tilde{q}(r,t) = q_2(h(r,t)) \sqrt{\frac{\partial h}{\partial (r,t)}(r,t)},\ (r,t) \in D,\ h \in \Gamma_D \Big\},$$

and $\tilde{q}_2$ in $[q_2]_{\Gamma_D}$ given by $\tilde{q}_2(r,t) = q_2(h^{(k)}(r,t)) \sqrt{\frac{\partial h^{(k)}}{\partial (r,t)}(r,t)}$, at the $(k+1)^{th}$ iteration of the approach, letting $T_{\tilde{q}_2}([q_2]_{\Gamma_D})$ be the tangent space to $[q_2]_{\Gamma_D}$ at $\tilde{q}_2$, $T_{h_{id}}(\Gamma_D)$ the tangent space to Γ_D at h_{id}, and ϕ the mapping from Γ_D into $[q_2]_{\Gamma_D}$ defined by $\phi(h)(r,t) = \tilde{q}_2(h(r,t)) \sqrt{\frac{\partial h}{\partial (r,t)}(r,t)}$, $(r,t) \in D$, $h \in \Gamma_D$, since $\phi(h_{id}) = \tilde{q}_2$, then the differential $d\phi_{h_{id}} : T_{h_{id}}(\Gamma_D) \to T_{\tilde{q}_2}([q_2]_{\Gamma_D})$ of ϕ at h_{id} can be defined. Accordingly, given v in $T_{h_{id}}(\Gamma_D)$, the lemma that follows

shows how to compute $d\phi_{h_{id}}(v)$, and using the result of this computation, the theorem that also follows shows how to compute at the $(k+1)^{th}$ iteration of the approach the directional derivative $\nabla_v H$ of H (actually $\nabla_v H_{k+1}$ of H_{k+1}) in the direction of v.

We note then that given w_i, $i = 1, 2, 3, \ldots$, an orthonormal basis of the vector space $T_{h_{id}}(\Gamma_D)$ under some metric, e.g., the basis presented in [12] which we describe later in this section, at the $(k+1)^{th}$ iteration of the approach the gradient of H_{k+1} is approximated by $\nabla H_{k+1} = \sum_{i=1}^{N} (\nabla_{w_i} H_{k+1}) w_i$, for N large enough. If under the same metric ∇H_{k+1} is considered to be small enough, then $h^{(k)}$ is taken to be the solution of the gradient descent approach, although perhaps a local solution. Otherwise, using a small step size $\delta > 0$, h_{k+1} and $h^{(k+1)}$ are computed, $h_{k+1} = h_{id} - \delta \ \nabla H_{k+1}$, $h^{(k+1)} = h^{(k)} \circ h_{k+1}$. That $h^{(k+1)}$ is computed so that $H(h^{(k+1)}) = H_{k+1}(h_{k+1})$ follows by letting $\tilde{q}_2$ be as obtained at the k^{th} iteration of the approach, and proving that

$$q_2(h^{(k+1)}(r,t))\sqrt{\frac{\partial h^{(k+1)}}{\partial(r,t)}(r,t)} = \tilde{q}_2(h_{k+1}(r,t))\sqrt{\frac{\partial h_{k+1}}{\partial(r,t)}(r,t)}, \ (r,t) \in D,$$

as follows:

$$\begin{aligned}
& \tilde{q}_2(h_{k+1}(r,t))\sqrt{\frac{\partial h_{k+1}}{\partial(r,t)}(r,t)} \\
= \ & q_2(h^{(k)}(h_{k+1}(r,t)))\sqrt{\frac{\partial h^{(k)}}{\partial(u,w)}(h_{k+1}(r,t))}\sqrt{\frac{\partial h_{k+1}}{\partial(r,t)}(r,t)} \\
= \ & q_2(h^{(k)}(h_{k+1}(r,t)))\sqrt{\frac{\partial h^{(k)}}{\partial(u,w)}(h_{k+1}(r,t))\frac{\partial h_{k+1}}{\partial(r,t)}(r,t)} \\
= \ & q_2(h^{(k+1)}(r,t))\sqrt{\frac{\partial h^{(k+1)}}{\partial(r,t)}(r,t)}
\end{aligned}$$

with $(u(r,t), w(r,t)) = h_{k+1}(r,t)$ by the product rule for determinants and the chain rule.

The lemma and theorem follow. Here shape functions are C^1 as well.

As above, given $h \in \Gamma_D$, in what follows $\frac{\partial h}{\partial(r,t)}$ is the determinant of the Jacobian of h, i.e., $\frac{\partial h}{\partial(r,t)} = \frac{\partial h_1}{\partial r}\frac{\partial h_2}{\partial t} - \frac{\partial h_1}{\partial t}\frac{\partial h_2}{\partial r}$, where $h(r,t) = (h_1(r,t), h_2(r,t))$, $(r,t) \in D$. Finally, given $h \in \Gamma_D$, again $h(r,t) = (h_1(r,t), h_2(r,t))$, and $v \in T_h(\Gamma_D)$, $v(r,t) = (v_1(r,t), v_2(r,t))$, $(r,t) \in D$, we define

$$\frac{\partial(v,h)}{\partial(r,t)} \equiv \frac{\partial v_1}{\partial r}\frac{\partial h_2}{\partial t} - \frac{\partial v_2}{\partial r}\frac{\partial h_1}{\partial t} + \frac{\partial h_1}{\partial r}\frac{\partial v_2}{\partial t} - \frac{\partial h_2}{\partial r}\frac{\partial v_1}{\partial t},$$

and let $\mathrm{div}(v)$ be the divergence of v, i.e., $\mathrm{div}(v)(r,t) = \frac{\partial v_1}{\partial r}(r,t) + \frac{\partial v_2}{\partial t}(r,t)$.

Lemma 2: Given q, the shape function of a surface in 3−dimensional space, $\phi : \Gamma_D \to [q]_{\Gamma_D}$, $\phi(h(r,t)) = q(h(r,t))\sqrt{\frac{\partial h}{\partial(r,t)}(r,t)}$, then given h in Γ_D, v in $T_h(\Gamma_D)$, with $\dot{q}$ the Jacobian of q, the differential of ϕ at h applied on v is

$$\begin{aligned}(d\phi_h(v))(r,t) &= \sqrt{\frac{\partial h}{\partial(r,t)}(r,t)}\dot{q}(h(r,t))v(r,t) + \\ &\frac{1}{2\sqrt{\frac{\partial h}{\partial(r,t)}(r,t)}}\frac{\partial(v,h)}{\partial(r,t)}(r,t)q(h(r,t)),\ (r,t) \in D.\end{aligned}$$

Proof: Let $\alpha(\tau,\cdot,\cdot)$ be a differentiable path in Γ_D passing through h at $\tau = 0$, i.e., $\alpha(0,r,t) = h(r,t)$, $(r,t) \in D$. Let the velocity of this path at $\tau = 0$ be given by $v \in T_h(\Gamma_D)$, i.e., $v(r,t) = \frac{\partial \alpha}{\partial \tau}(0,r,t)$, $(r,t) \in D$. Note as well, with $\alpha(\tau,r,t) = (\alpha_1(\tau,r,t), \alpha_2(\tau,r,t))$, and again with $h(r,t) = (h_1(r,t), h_2(r,t))$, $v(r,t) = (v_1(r,t), v_2(r,t))$, that

$$\begin{aligned}\frac{\partial \alpha_1}{\partial r}(0,r,t) &= \frac{\partial h_1}{\partial r}(r,t), \quad \frac{\partial \alpha_1}{\partial t}(0,r,t) = \frac{\partial h_1}{\partial t}(r,t), \\ \frac{\partial \alpha_2}{\partial r}(0,r,t) &= \frac{\partial h_2}{\partial r}(r,t), \quad \frac{\partial \alpha_2}{\partial t}(0,r,t) = \frac{\partial h_2}{\partial t}(r,t),\end{aligned}$$

$$\begin{aligned}\frac{\partial^2 \alpha_1}{\partial r \partial \tau}(0,r,t) &= \frac{\partial v_1}{\partial r}(r,t), \quad \frac{\partial^2 \alpha_1}{\partial t \partial \tau}(0,r,t) = \frac{\partial v_1}{\partial t}(r,t), \\ \frac{\partial^2 \alpha_2}{\partial r \partial \tau}(0,r,t) &= \frac{\partial v_2}{\partial r}(r,t), \quad \frac{\partial^2 \alpha_2}{\partial t \partial \tau}(0,r,t) = \frac{\partial v_2}{\partial t}(r,t), \quad (r,t) \in D.\end{aligned}$$

Since

$$\frac{\partial \alpha}{\partial(r,t)}(\tau,r,t) = \frac{\partial \alpha_1}{\partial r}(\tau,r,t)\frac{\partial \alpha_2}{\partial t}(\tau,r,t) - \frac{\partial \alpha_2}{\partial r}(\tau,r,t)\frac{\partial \alpha_1}{\partial t}(\tau,r,t),$$

it follows then that

$$\begin{aligned}\frac{\partial\alpha}{\partial(r,t)}(\tau,r,t)|_{\tau=0} &= \frac{\partial\alpha_1}{\partial r}(0,r,t)\frac{\partial\alpha_2}{\partial t}(0,r,t) - \frac{\partial\alpha_2}{\partial r}(0,r,t)\frac{\partial\alpha_1}{\partial t}(0,r,t)\\ &= \frac{\partial h_1}{\partial r}(r,t)\frac{\partial h_2}{\partial t}(r,t) - \frac{\partial h_2}{\partial r}(r,t)\frac{\partial h_1}{\partial t}(r,t)\\ &= \frac{\partial h}{\partial(r,t)}(r,t).\end{aligned}$$

In addition, we note that

$$\begin{aligned}&\frac{\partial}{\partial\tau}\big(\frac{\partial\alpha}{\partial(r,t)}(\tau,r,t)\big)|_{\tau=0}\\ =\ &\frac{\partial}{\partial\tau}\big(\frac{\partial\alpha_1}{\partial r}(\tau,r,t)\frac{\partial\alpha_2}{\partial t}(\tau,r,t) - \frac{\partial\alpha_2}{\partial r}(\tau,r,t)\frac{\partial\alpha_1}{\partial t}(\tau,r,t)\big)|_{\tau=0}\\ =\ &\big(\frac{\partial^2\alpha_1}{\partial\tau r}(\tau,r,t)\frac{\partial\alpha_2}{\partial t}(\tau,r,t) + \frac{\partial\alpha_1}{\partial r}(\tau,r,t)\frac{\partial^2\alpha_2}{\partial\tau t}(\tau,r,t)\\ &-\frac{\partial^2\alpha_2}{\partial\tau r}(\tau,r,t)\frac{\partial\alpha_1}{\partial t}(\tau,r,t) - \frac{\partial\alpha_2}{\partial r}(\tau,r,t)\frac{\partial^2\alpha_1}{\partial\tau t}(\tau,r,t)\big)|_{\tau=0}\\ =\ &\big(\frac{\partial^2\alpha_1}{\partial r\tau}(\tau,r,t)\frac{\partial\alpha_2}{\partial t}(\tau,r,t) + \frac{\partial\alpha_1}{\partial r}(\tau,r,t)\frac{\partial^2\alpha_2}{\partial t\tau}(\tau,r,t)\\ &-\frac{\partial^2\alpha_2}{\partial r\tau}(\tau,r,t)\frac{\partial\alpha_1}{\partial t}(\tau,r,t) - \frac{\partial\alpha_2}{\partial r}(\tau,r,t)\frac{\partial^2\alpha_1}{\partial t\tau}(\tau,r,t)\big)|_{\tau=0}\\ =\ &\frac{\partial v_1}{\partial r}(r,t)\frac{\partial h_2}{\partial t}(r,t) + \frac{\partial h_1}{\partial r}(r,t)\frac{\partial v_2}{\partial t}(r,t)\\ &-\frac{\partial v_2}{\partial r}(r,t)\frac{\partial h_1}{\partial t}(r,t) - \frac{\partial h_2}{\partial r}(r,t)\frac{\partial v_1}{\partial t}(r,t)\\ =\ &\frac{\partial(v,h)}{\partial(r,t)}(r,t).\end{aligned}$$

Since $\alpha(\tau,\cdot,\cdot)$ is a path in Γ_D, then $\phi(\alpha(\tau,\cdot,\cdot))$ is the corresponding path in $[q]_{\Gamma_D}$, and since v is the velocity of $\alpha(\tau,\cdot,\cdot)$ at $\tau = 0$, then the velocity of $\phi(\alpha(\tau,\cdot,\cdot))$ at $\tau = 0$ is $d\phi_h(v)$,

that is to say

$$(d\phi_h(v))(r,t) = \frac{\partial}{\partial\tau}|_{\tau=0}\ \phi(\alpha(\tau,r,t))$$

$$
\begin{aligned}
&= \frac{\partial}{\partial\tau}|_{\tau=0}\Big(\sqrt{\frac{\partial\alpha}{\partial(r,t)}(\tau,r,t)}\; q(\alpha(\tau,r,t))\Big)\\
&= \Big(\sqrt{\frac{\partial\alpha}{\partial(r,t)}(\tau,r,t)}\; \dot{q}(\alpha(\tau,r,t))\; \frac{\partial\alpha}{\partial\tau}(\tau,r,t)\; +\\
&\quad \frac{1}{2\sqrt{\frac{\partial\alpha}{\partial(r,t)}(\tau,r,t)}}\; \frac{\partial}{\partial\tau}\big(\frac{\partial\alpha}{\partial(r,t)}(\tau,r,t)\big)\; q(\alpha(\tau,r,t))\Big)|_{\tau=0}\\
&= \sqrt{\frac{\partial h}{\partial(r,t)}(r,t)}\dot{q}(h(r,t))v(r,t)\; +\\
&\quad \frac{1}{2\sqrt{\frac{\partial h}{\partial(r,t)}(r,t)}}\frac{\partial(v,h)}{\partial(r,t)}(r,t)q(h(r,t)),\;\; (r,t)\in D.
\end{aligned}
$$

□

Corollary 2: Given q, ϕ, v as above, then

$$(d\phi_{h_{id}}(v))(r,t) = \dot{q}(r,t)v(r,t) + \frac{1}{2}\mathrm{div}(v)(r,t)q(r,t),\;\; (r,t)\in D.$$

Theorem 2: With $H_{k+1}(h) = \int_0^1\int_0^1 ||q_1(r,t) - \tilde{q}_2(h(r,t))\sqrt{\frac{\partial h}{\partial(r,t)}(r,t)}||^2\; dr\; dt$ so that $\tilde{q}_2(r,t) = q_2(h^{(k)}(r,t))\sqrt{\frac{\partial h^{(k)}}{\partial(r,t)}(r,t)}$ from the definition of H_{k+1}, then the directional derivative of H_{k+1} in the direction of $v\in T_{h_{id}}(\Gamma_D)$ is

$$
\begin{aligned}
\nabla_v H_{k+1} &= -2\int_0^1\int_0^1 \Big\langle q_1(r,t) - \tilde{q}_2(r,t)\;,\\
&\qquad \dot{\tilde{q}}_2(r,t)v(r,t) + \frac{1}{2}\mathrm{div}(v)(r,t)\tilde{q}_2(r,t)\Big\rangle\; dr\; dt.
\end{aligned}
$$

Proof: Let $\alpha(\tau,\cdot,\cdot)$ be a differentiable path in Γ_D passing through h_{id} at $\tau = 0$, i.e., $\alpha(0,r,t) = h_{id}(r,t)$, $(r,t)\in D$, with the velocity of this path at $\tau = 0$ equal to v, i.e., $\frac{\partial\alpha}{\partial\tau}(0,r,t) = v(r,t)$, $(r,t)\in D$.

Note,

$$H_{k+1}(\alpha(\tau,r,t)) = \int_0^1\int_0^1 \Big\langle q_1(r,t) - \tilde{q}_2(\alpha(\tau,r,t))\sqrt{\frac{\partial\alpha}{\partial(r,t)}(\tau,r,t)}\;,$$

$$q_1(r,t) - \tilde{q}_2(\alpha(\tau,r,t))\sqrt{\frac{\partial\alpha}{\partial(r,t)}(\tau,r,t)}\Big\rangle \; dr \; dt.$$

Again, since in general $\frac{d}{ds}\langle f(s), g(s)\rangle = \langle f(s), g'(s)\rangle + \langle f'(s), g(s)\rangle$, from which $\frac{d}{ds}\langle f(s), f(s)\rangle = 2\langle f(s), f'(s)\rangle$, then differentiating $H_{k+1}(\alpha(\tau,r,t))$ with respect to τ by differentiating this last integral with respect to τ (done under the integral), and setting τ equal to zero, gives

$$\begin{aligned}
\nabla_v H_{k+1} &= 2\int_0^1\int_0^1 \Big\langle q_1(r,t) - \tilde{q}_2(h_{id}(r,t))\sqrt{\frac{\partial h_{id}}{\partial(r,t)}(r,t)}\,, \\
&\quad \frac{\partial}{\partial\tau}|_{\tau=0}\Big(- \tilde{q}_2(\alpha(\tau,r,t))\sqrt{\frac{\partial\alpha}{\partial(r,t)}(\tau,r,t)}\Big)\Big\rangle \; dr \; dt \\
&= -2\int_0^1\int_0^1 \Big\langle q_1(r,t) - \tilde{q}_2(r,t)\,, \\
&\quad \frac{\partial}{\partial\tau}|_{\tau=0}\Big(\tilde{q}_2(\alpha(\tau,r,t))\sqrt{\frac{\partial\alpha}{\partial(r,t)}(\tau,r,t)}\Big)\Big\rangle \; dr \; dt \\
&= -2\int_0^1\int_0^1 \Big\langle q_1(r,t) - \tilde{q}_2(r,t)\,, \\
&\quad \dot{\tilde{q}}_2(r,t)v(r,t) + \frac{1}{2}\mathrm{div}(v)(r,t)\tilde{q}_2(r,t)\Big\rangle \; dr \; dt
\end{aligned}$$

by Corollary 2 and the proof of Lemma 2 as α here is the same as α there with h equal to h_{id}. □

Note that given $h \in \Gamma_D$ and a differentiable path $\alpha(\tau,\cdot,\cdot)$ in Γ_D through h at $\tau = 0$, i.e., $\alpha(0,r,t) = h(r,t)$, $(r,t) \in D$, then with $\alpha(\tau,r,t) = (\alpha_1(\tau,r,t), \alpha_2(\tau,r,t))$, since for any real numbers τ_1, τ_2, close or equal to 0, for $0 \le r,t \le 1$, $\alpha_1(\tau_1,0,t) - \alpha_1(\tau_2,0,t) = 0-0 = 0$, $\alpha_2(\tau_1,r,0) - \alpha_2(\tau_2,r,0) = 0-0 = 0$, $\alpha_1(\tau_1,1,t) - \alpha_1(\tau_2,1,t) = 1-1 = 0$, $\alpha_2(\tau_1,r,1) - \alpha_2(\tau_2,r,1) = 1-1 = 0$, with $v(r,t) = (v_1(r,t), v_2(r,t))$, $(r,t) \in D$, $v \in T_h(\Gamma_D)$, it can also be shown that

$$\begin{aligned}
T_h(\Gamma_D) &= \{v : D \to \mathbb{R}^2 \mid v_1(0,t) = v_2(r,0) = v_1(1,t) = v_2(r,1) = 0, \\
&\qquad 0 \le r,t \le 1,\ v \text{ smooth}\}.
\end{aligned}$$

Next, we present and describe the orthonormal basis under the L^2 norm of the vector space $T_{h_{id}}(\Gamma_D)$ presented in [12] as it is the basis we use as well.

As described in [12], first an orthonormal basis B^1 under the L^2 norm is identified for the space

$$S^r_{rt} = \{v : D \to \mathbb{R} \mid v(0,t) = v(1,t) = 0,\ 0 \le t \le 1,\ v \text{ smooth}\}$$

that consists of three families of functions: $\sqrt{2}\sin(\pi kr)$, $2\sin(\pi kr)\cos(2\pi lt)$, $2\sin(\pi kr)\sin(2\pi lt)$, $k, l = 1, 2, 3, \ldots$, $(r,t) \in D$.

With one$(t) = 1$ for all $t,\ 0 \le t \le 1$, using $\phi_m(r)$, $m = 1, 2, 3, \ldots$, to refer to $\sqrt{2}\sin(\pi kr)$, $0 \le r \le 1$, $k = 1, 2, 3, \ldots$, and $\psi_n(t)$, $n = 1, 2, 3, \ldots$, to refer to one(t), $\sqrt{2}\cos(2\pi lt)$, $\sqrt{2}\sin(2\pi lt)$, $0 \le t \le 1$, $l = 1, 2, 3, \ldots$, then under the L^2 norm ϕ_m, $m = 1, 2, 3, \ldots$, is an orthonormal basis for the space

$$\{v : [0,1] \to \mathbb{R} \mid v(0) = v(1) = 0,\ v \text{ smooth}\}$$

and ψ_n, $n = 1, 2, 3, \ldots$, is an orthonormal basis for the space

$$\{v : [0,1] \to \mathbb{R} \mid v \text{ smooth}\}.$$

Clearly B^1 is the tensor product of the two bases ϕ_m, $m = 1, 2, 3 \ldots$, and ψ_n, $n = 1, 2, 3, \ldots$, and that B_1 is linearly independent is a direct result of the linear independence of these two bases. Finally, given $v \in S^r_{rt}$, that v is a linear combination, possibly infinite under the L^2 norm, of elements of B_1, is established by applications of Parseval's identity (three times) together with Fubini's theorem (twice) as follows:

$$\sum_{m,n} \Big| \int\int_D v(r,t)\phi_m(r)\psi_n(t)drdt \Big|^2 = \sum_{m,n} \Big| \int_0^1 \Big(\int_0^1 v(r,t)\phi_m(r)dr \Big)\psi_n(t)dt \Big|^2$$

$$\begin{aligned} &= \sum_m \int_0^1 \Big| \int_0^1 v(r,t)\phi_m(r)dr \Big|^2 dt = \int_0^1 \sum_m \Big| \int_0^1 v(r,t)\phi_m(r)dr \Big|^2 dt \\ &= \int_0^1 \Big(\int_0^1 \Big| v(r,t) \Big|^2 dr \Big) dt = \int\int_D \Big| v(r,t) \Big|^2 drdt. \end{aligned}$$

Similarly, an orthonormal basis B^2 under the L^2 norm can be identified and justified for the space

$$S^t_{rt} = \{v : D \to \mathbb{R} \mid v(r,0) = v(r,1) = 0,\ 0 \le r \le 1,\ v \text{ smooth}\}$$

that consists of three families of functions: $\sqrt{2}\sin(\pi kt)$, $2\sin(\pi kt)\cos(2\pi lr)$, $2\sin(\pi kt)\sin(2\pi lr)$, $k, l = 1, 2, 3, \ldots$, $(r, t) \in D$.

Using $\eta_j(r, t)$, $j = 1, 2, 3, \ldots$, to refer to the elements of the basis B^1 of S^r_{rt}, i.e., to $\sqrt{2}\sin(\pi kr)\text{one}(t)$, $2\sin(\pi kr)\cos(2\pi lt)$, $2\sin(\pi kr)\sin(2\pi lt)$, $k, l = 1, 2, 3, \ldots$, $(r, t) \in D$, it is clear then that $\eta_j(t, r)$, $j = 1, 2, 3, \ldots$, $(r, t) \in D$, are the elements of the basis B^2 of S^t_{rt}. Note as well that if for some integer $KL > 0$ we restrict k, l above to range from 1 to KL, then j above in the definition of η_j will range from 1 to $KL + 2(KL)^2$.

With $\text{zero}(r, t) = 0$ for all $(r, t) \in D$, then as in [12] an orthonormal basis B of $T_{h_{id}}(\Gamma_D)$ under the L^2 norm can be identified:

$$B = \{(\eta_j(r, t), \text{zero}(r, t)), (\text{zero}(r, t), \eta_j(t, r)), j = 1, 2, 3, \ldots, (r, t) \in D\}.$$

We note that under the identification of $T_h(\Gamma_D)$ given above following the proof of Theorem 2, each element of B is indeed in $T_{h_{id}}(\Gamma_D)$. We also note that with KL as above so that k, l above are restricted to range from 1 to KL, and j above in the definition of η_j is therefore restricted to range from 1 to $KL + 2(KL)^2$, if in the definition above of the basis B, j is restricted as well to range from 1 to $KL+2(KL)^2$, then B is truncated to have $2(KL+2(KL)^2)$ elements.

Next, we present a simplified outline of the procedure for the elastic shape registration of two surfaces in $3-$dimensional space using gradient descent and dynamic programming. Note that in the procedure a step size $\delta > 0$ is used for computing elements of Γ_D, the computation of δ discussed below, δ as large as the gradient descent approach allows but small enough to guarantee that each computed element of Γ_D is indeed in Γ_D, in particular that the determinant of its Jacobian is positive everywhere on D. We note as well that in this simplified outline of the procedure, rotations are also taken into account as they should be, so that it is

$$E(h, R) = \int_0^1 \int_0^1 \Big|\Big|Rq_1 - (q_2 \circ h)\sqrt{\frac{\partial h}{\partial(r, t)}}\Big|\Big|^2 dr\, dt$$

that we actually hope to minimize with respect to $h \in \Gamma_D$ and $R \in SO(3)$. Here we use w_i, $i = 1, 2, 3, \ldots$, to refer to the elements of the basis B.

Simplified Outline of Optimization Procedure

1. With q_1, q_2 as the shape functions of the two simple surfaces under consideration, say S_1 and S_2, execute dynamic-programming-based Procedure DP-surface-min in [3] for q_1, q_2, to obtain (partially) optimal $\hat{R} \in SO(3)$ and $h_0 \in \Gamma_D$, where $\hat{R}$ rotates S_1 and h_0 reparametrizes S_2.
Set $k = 0$, $h^{(0)} = h_0$.
Compute $\hat{q}_1 = \hat{R}q_1$, $\tilde{q}_2 = (q_2, h^{(0)}) = (q_2 \circ h^{(0)})\sqrt{\frac{\partial h^{(0)}}{\partial(r,t)}}$,
and $E(h^{(0)}, \hat{R}) = \int_0^1 \int_0^1 ||\hat{q}_1 - \tilde{q}_2||^2 dr\, dt$.
If $E(h^{(0)}, \hat{R})$ is equal or close to zero, then go to Step 4 below.
Set N to a positive integer large enough.
2. For each i, $i = 1, \ldots, N$, compute $\nabla_{w_i} H_{k+1} =$
$-2 \int_0^1 \int_0^1 \left\langle \hat{q}_1(r,t) - \tilde{q}_2(r,t)\ ,\ \dot{\tilde{q}}_2(r,t) w_i(r,t) + \frac{1}{2}\mathrm{div}(w_i)(r,t)\tilde{q}_2(r,t) \right\rangle dr\ dt$
as indicated by Theorem 2 above, and compute $\nabla H_{k+1} = \sum_{i=1}^{N} (\nabla_{w_i} H_{k+1}) w_i$.
If the L^2 norm of ∇H_{k+1} is small enough, then go to Step 3 below.
Else for $\delta > 0$ appropriately chosen, set $h_{k+1} = h_{id} - \delta\, \nabla H_{k+1}$,
$h^{(k+1)} = h^{(k)} \circ h_{k+1}$, and $k = k + 1$.
Compute $\tilde{q}_2 = (q_2, h^{(k)}) = (q_2 \circ h^{(k)})\sqrt{\frac{\partial h^{(k)}}{\partial(r,t)}}$,
and $E(h^{(k)}, \hat{R}) = \int_0^1 \int_0^1 ||\hat{q}_1 - \tilde{q}_2||^2 dr\, dt$.
If $E(h^{(k)}, \hat{R})$ is equal or close to zero, then set $h_0 = h^{(k)}$ and go to Step 4 below.
If $E(h^{(k)}, \hat{R})$ is not much less than $E(h^{(k-1)}, \hat{R})$, then go to Step 3 below.
Else repeat this step (Step 2).
3. Set $h_0 = h^{(k)}$, $E_L = E(h^{(k)}, \hat{R})$.
With S_1, S_2 as above, execute KU3 algorithm in [3], that is, the Kabsch-Umeyama algorithm [8, 9, 11, 15], for $\tilde{q}_2$, q_1, to obtain optimal $\hat{R} \in SO(3)$ for the rigid alignment of S_1 and $\tilde{S}_2$, where $\hat{R}$ rotates S_1, and $\tilde{S}_2$ is S_2 reparametrized so that $\tilde{q}_2$ is its shape function.
Compute $\hat{q}_1 = \hat{R}q_1$, and $E(h_0, \hat{R}) = \int_0^1 \int_0^1 ||\hat{q}_1 - \tilde{q}_2||^2 dr\, dt$.
If $E(h_0, \hat{R})$ is equal or close to zero, then go to Step 4 below.
If this step (Step 3) has been executed enough times or $E(h_0, \hat{R})$ is not much less than E_L, then go to Step 4 below.
Else set $k = 0$, $h^{(0)} = h_0$.
Go to Step 2 above.
4. $h = h_0$ and $R = \hat{R}$ minimize $E(h, R)$, possibly resulting in a local solution.

If not a local solution, then $E(h_0, \hat{R})^{1/2}$ is the elastic shape distance between the two surfaces.
Stop.

Finally, we discuss how the step size $\delta > 0$ mentioned above for computing elements of Γ_D is chosen. This is done in a way similar to what is done in [12]. In particular, in Step 2 of the simplified outline of the optimization procedure above, h_{k+1} is computed as $h_{id} - \delta \nabla H_{k+1}$ so that $\delta > 0$ should be as large as the gradient descent approach allows but small enough that the determinant of the Jacobian of h_{k+1} is positive at every (r, t) in D, i.e., $\frac{\partial h_{k+1}}{\partial(r,t)}(r, t) > 0$ for each $(r, t) \in D$.

Let $A(r, t)$ be the 2×2 matrix which is the Jacobian of $\nabla H_{k+1}(r, t)$, $(r, t) \in D$. It then follows that the Jacobian of $h_{k+1}(r, t) = (h_{id} - \delta \nabla H_{k+1})(r, t)$, $(r, t) \in D$, is a 2×2 matrix as well equal to $I_2 - \delta A(r, t)$, where I_2 is the 2×2 identity matrix. Thus, it is not hard to show that

$$\frac{\partial h_{k+1}}{\partial(r,t)}(r, t) = 1 - \mathrm{tr}(A(r, t))\,\delta + \det(A(r, t))\,\delta^2, \quad (r, t) \in D,$$

where tr stands for trace and det for determinant.

For each $(r, t) \in D$, we hope to compute $\delta(r, t)$, which is the largest positive number for which $\frac{\partial h_{k+1}}{\partial(r,t)}(r, t) > 0$ for δ in the interval $(0, \delta(r, t))$, $\delta(r, t)$ possibly equal to ∞. With $a = \det A(r, t)$, $b = -\mathrm{tr}A(r, t)$, $c = 1$, if a is zero or close to zero, then it is not hard to show that $\delta(r, t)$ is approximately $-1/b$ if $b < 0$, ∞ otherwise. On the other hand, if a is not close to zero, then applying the quadratic formula it is not hard to show that $\delta(r, t)$ equals $\frac{-b-\sqrt{b^2-4a}}{2a}$ if this last number is a positive real number, ∞ otherwise.

Ideally we would like to be able to compute $\delta_{min} = \min_{(r,t)\in D} \delta(r, t)$, and if this number is positive, identify as the desired step size δ a positive number slightly less than δ_{min} so that $\frac{\partial h_{k+1}}{\partial(r,t)}(r, t) > 0$ for every $(r, t) \in D$. However, since as pointed out in [3], in practice we can only work with a discretization of D, minimizing $\delta(r, t)$ over D is a moot point, and in fact we assume that positive integers K, L, not necessarily equal, and partitions of $[0, 1]$, $\{r_i\}_{i=1}^K$, $r_1 = 0 < r_2 < \ldots < r_K = 1$, $\{t_j\}_{j=1}^L$, $t_1 = 0 < t_2 < \ldots <$

$t_L = 1$, not necessarily uniform, are given, so that it is the grid G on D, $G = \{(r_i, t_j), i = 1, \ldots, K,\ j = 1, \ldots, L\}$ that is actually used instead of D to identify the desired step size δ, i.e., we compute δ_{min} as $\min_{(r,t)\in G} \delta(r,t)$ instead, still identifying as the desired step size δ a positive number slightly less than δ_{min}.

At the risk of making the step size δ too small, we may reduce the step size computed as suggested above, to make sure that indeed h_{k+1} is one to one and maps D onto D, while maintaining the boundary conditions of elements of Γ_D. For this purpose we take advantage of the Gale-Nikaido Theorem [5] that follows. Here, given integer $n > 0$, real numbers $a_i,\ b_i,\ i = 1, \ldots, n$, some or all of them allowed to be $-\infty$ or ∞, a rectangular region R in $\mathbb{R}^n$ is defined by

$$R = \{x : x \in \mathbb{R}^n,\ x = (x_1, \ldots, x_n) \text{ with } a_i \le x_i \le b_i,\ i = 1, \ldots, n\}.$$

Theorem 3: (Gale-Nikaido Theorem) If F is a C^1 mapping from a rectangular region R in $\mathbb{R}^n$ into $\mathbb{R}^n$ such that for all $x \in R$ each principle minor of the Jacobian matrix of F at x is positive, then F is injective.

Accordingly, for each $(r,t) \in D$, with $a_{ij}(r,t)$, $i, j = 1, 2$, the entries of $A(r,t)$, $A(r,t)$ as above, it is not hard to see that for our purposes the minors of interest of the Jacobian matrix of h_{k+1} at (r,t) are $\frac{\partial h_{k+1}}{\partial(r,t)}(r,t)$, $1 - \delta\, a_{11}(r,t)$ and $1 - \delta\, a_{22}(r,t)$, and the goal is then to compute $\hat{\delta}(r,t)$, which is the largest positive number for which all three minors are positive for δ in the interval $(0, \hat{\delta}(r,t))$, $\hat{\delta}(r,t)$ possibly equal to ∞. Again with G as above, we work with G instead of D, and note that for $(r,t) \in G$, $\frac{\partial h_{k+1}}{\partial(r,t)}(r,t)$ has already been taken care of above during the computation of δ_{min}. Thus, for each $(r,t) \in G$, we compute $\hat{\delta}(r,t)$ only with respect to $1 - \delta\, a_{11}(r,t)$ and $1 - \delta\, a_{22}(r,t)$ as follows. If both $a_{11}(r,t)$ and $a_{22}(r,t)$ are nonpositive, then $\hat{\delta}(r,t)$ equals ∞. If both $a_{11}(r,t)$ and $a_{22}(r,t)$ are positive, then $\hat{\delta}(r,t)$ is the smaller of $1/a_{11}(r,t)$ and $1/a_{22}(r,t)$. Otherwise, only one of $a_{11}(r,t)$ and $a_{22}(r,t)$ is positive, and $\hat{\delta}(r,t)$ is 1 divided by the one of the two that is positive. Having done this for each $(r,t) \in G$, with δ_{min} as computed above, and $\hat{\delta}_{min} = \min_{(r,t)\in G} \hat{\delta}(r,t)$, we identify as the desired step size δ a positive number slightly less than the smaller of δ_{min} and $\hat{\delta}_{min}$, and assume for all intents and purposes that with this δ the determinant of the Jacobian of h_{k+1} is positive on D, and since D is the unit square, thus a rectangular region, that h_{k+1} is one to

one on D by the Gale-Nikaido Theorem above. In addition, since we assume $\frac{\partial h_{k+1}}{\partial(r,t)}(r,t) > 0$ on D, thus nonzero, by the inverse function theorem we may assume the inverse of h_{k+1} is a C^1 function.

Assuming then that h_{k+1} is a one-to-one C^1 function on all of D with a C^1 inverse, we show that h_{k+1} maps D onto D. For this purpose we need the two well-known results that follow. Here a homeomorphism is a one-to-one continuous function from a topological space onto another that has a continuous inverse function, and a simply connected domain is a path-connected domain where one can continuously shrink any simple closed curve into a point while remaining in the domain. For two-dimensional regions, a simply connected domain is one without holes in it. The two results appeared in [3], the first result a standard result in the field of topology, the proof of the second result presented in [3] for the sake of completeness.

Theorem 4: If X and Y are homeomorphic topological spaces, then X is simply connected if and only if Y is simply connected.

Theorem 5: Given E, a compact simply connected subset of $\mathbb{R}^2$, and $h : E \to \mathbb{R}^2$, a homeomorphism, then h maps the boundary of E to exactly the boundary of $h(E)$.

From these two theorems it then follows that $h_{k+1}(D)$ is simply connected and that h_{k+1} maps the boundary of D to exactly the boundary of $h_{k+1}(D)$. Note, in particular, the boundary of $h_{k+1}(D)$ is then contained in $h_{k+1}(D)$.

Note, from the definition of h_{k+1}, that $h_{k+1}(0,0) = (0,0)$, $h_{k+1}(0,1) = (0,1)$, $h_{k+1}(1,1) = (1,1)$, $h_{k+1}(1,0) = (1,0)$. In particular, given r, $0 < r < 1$, then again from the definition of h_{k+1}, $h_{k+1}(r,1) = (r',1)$, r' a number not necessarily between 0 and 1, so that $h_{k+1}(r,1)$ is in the line $t = 1$ which contains the line segment with endpoints $(0,1)$, $(1,1)$, i.e., the top side of the unit square D. However this line segment is connected, so that its image under h_{k+1} in the line $t = 1$ is connected and thus must contain the line segment, and since h_{k+1} is one to one, this image is exactly the line segment. Since the same is true for the other three sides of D, then it follows that the boundary conditions of elements of Γ_D are satisfied by h_{k+1}, and that h_{k+1} actually maps the boundary of D onto itself. However, we already know that

h_{k+1} maps the boundary of D to exactly the boundary of $h_{k+1}(D)$, thus the boundary of D and the boundary of $h_{k+1}(D)$ are exactly the same. Since D and $h_{k+1}(D)$ are both simply connected, then $h_{k+1}(D) = D$.

5 Results from Implementation of Methods

A software package has been implemented that incorporates the methods presented in the previous section for computing, using gradient descent and dynamic programming, the elastic shape registration of two simple surfaces in 3−dimensional space, and therefore the elastic shape distance between them. Actually, the software package consists of two separate pieces of software. One piece is based on gradient descent as presented in the previous section for reparametrizing one of the surfaces. This piece uses as the input initial solution the rotation and reparametrization computed with the other piece of sofware in the package which is based on dynamic programming as presented in [3] for reparametrizing one of the surfaces to obtain a partial elastic shape registration of the surfaces. As described in [3], the software in the package based on dynamic programming is in Matlab[1] with the exception of the dynamic programming routine which is written in Fortran but is executed as a Matlab mex file. On the other hand, the software in the package based on gradient descent is entirely in Matlab. In this section, we present results obtained from executions of the software package. We note, the software package as well as input data files, a README file, etc. can be obtained at the following link

`http://math.nist.gov/~JBernal /ESD_surf_gradesc.zip`

We note, Matlab routine ESD_main_surf_3d.m is the driver routine of the package, and Fortran routine DP_MEX_WNDSTRP_ALLDIM.F is the dynamic programming routine in the software based on dynamic programming. This routine has already been processed to be executed as a Matlab mex file. In case the Fortran routine must be processed to obtain a new mex file, this can be done by typing in the Matlab window:
mex - compatibleArrayDims DP_MEX_WNDSTRP_ALLDIM.F

As was the case for the software package described in [3], at the start of

[1]The identification of any commercial product or trade name does not imply endorsement or recommendation by the National Institute of Standards and Technology.

the execution of the new software package based on gradient descent and dynamic programming that we are describing here, we assume S_1, S_2 are the two simple surfaces in 3−dimensional space under consideration, with functions c_1, $c_2 : D \equiv [0, T_1] \times [0, T_2] \to \mathbb{R}^3$, T_1, $T_2 > 0$, as their parametrizations, respectively, so that $S_1 = c_1(D)$, $S_2 = c_2(D)$. We also assume that as input to the software, for positive integers M, N, not necessarily equal, and partitions of $[0, T_1]$, $[0, T_2]$, respectively, $\{r_i\}_{i=1}^M$, $r_1 = 0 < r_2 < \ldots < r_M = T_1$, $\{t_j\}_{j=1}^N$, $t_1 = 0 < t_2 < \ldots < t_N = T_2$, not necessarily uniform, discretizations of c_1, c_2 are given, each discretization in the form of a list of $M \times N$ points in the corresponding surface, namely $c_1(r_i, t_j)$ and $c_2(r_i, t_j)$, $i = 1, \ldots, M$, $j = 1, \ldots, N$, respectively, and for each k, $k = 1, 2$, as specified in the Introduction section in [3], in the order $c_k(r_1, t_1)$, $c_k(r_2, t_1)$, ..., $c_k(r_M, t_1)$, ..., $c_k(r_1, t_N)$, $c_k(r_2, t_N)$, ..., $c_k(r_M, t_N)$. Based on this input, for the purpose of computing, using dynamic programming, a partial elastic shape registration of S_1 and S_2, together with the elastic shape distance between them associated with the partial registration, the program always proceeds first to scale the partitions $\{r_i\}_{i=1}^M$, $\{t_j\}_{j=1}^N$, so that they become partitions of $[0, 1]$, and to compute an approximation of the area of each surface. During the execution of the software package, the former is accomplished by the driver routine Matlab routine ESD_main_surf_3d.m, while the latter by Matlab routine ESD_comp_surf_3d.m (called by ESD_main_surf_3d.m) through the computation for each k, $k = 1, 2$ of the sum of the areas of triangles with vertices $c_k(r_i, t_j)$, $c_k(r_{i+1}, t_{j+1})$, $c_k(r_i, t_{j+1})$, and $c_k(r_i, t_j)$, $c_k(r_{i+1}, t_j)$, $c_k(r_{i+1}, t_{j+1})$, for $i = 1, \ldots, M-1$, $j = 1, \ldots, N-1$. This last routine then proceeds to scale the discretizations of the parametrizations of the two surfaces so that each surface has approximate area equal to 1 (given a surface and its approximate area, each point in the discretization of the parametrization of the surface is divided by the square root of half the approximate area of the surface). Once routine ESD_comp_surf_3d.m is done with these computations, the actual computations of the rotation and reparametrization based on dynamic programming for reparametrizing one of the surfaces to obtain a partial elastic shape registration of the surfaces, are carried out by Matlab routine ESD_core_surf_3d.m (called by ESD_comp_surf_3d.m) in which the methods for this purpose presented in [3], mainly Procedure DP-surface-min in Section 7 of [3], have been implemented. Note, it is in this routine that the dynamic programming routine Fortran routine DP_MEX_WNDSTRP_ALLDIM.F is executed. Finally, Matlab routine ESD_grad_surf_3d.m (called by ESD_main_surf_3d.m) is

executed for the purpose of computing, using gradient descent, the elastic shape registration of the two surfaces, together with the elastic shape distance between them. Note, this routine uses as the input initial solution the rotation and reparametrization computed by routine ESD_core_surf_3d.m that as part of the output of ESD_comp_surf_3d.m become available for ESD_grad_surf_3d.m to use as input. Note as well that in this routine with integer $KL > 0$ and infinite basis B, KL and B as defined in the previous section, we use $KL = 5$ so that the basis B is then truncated to have $2(KL + 2(KL)^2) = 110$ elements.

The results that follow were obtained from applications of our software package on discretizations of the three kinds of surfaces in 3−dimensional space that were identified in [3] and that were called there surfaces of the sine, helicoid and cosine-sine kind. Of course results in [3] were obtained using software based on dynamic programming only on the aforementioned discretizations, while here results were obtained through executions of our software package, using software based on both dynamic programming and gradient descent, used separately and combined (by setting variable insol equal to 1 in the driver routine Matlab routine ESD_main_surf_3d.m, gradient descent is used with initial solution the rotation and diffeomorphism computed with dynamic programming; otherwise, gradient descent is used with initial solution the identity matrix and the identity diffeomorphism; note, with a couple of exceptions, the results reported here obtained with the software package using dynamic programming before using gradient descent are the same as the results reported in [3], with comments given there about these results still valid for the resuts here). As was the case when using software based on dynamic programming only as described in [3], when using our software package, on input all surfaces were given as discretizations on the unit square ($[0,1] \times [0,1]$), each interval $[0,1]$ uniformly partitioned into 100 intervals so that the unit square was thus partitioned into 10000 squares, each square of size 0.01×0.01, their corners making up a set of 10201 points. Using the same notation used above in this section, the uniform partitions of the two $[0,1]$ intervals that define the unit square were then $\{r_i\}_{i=1}^M$, $\{t_j\}_{j=1}^N$, with $M = N = 101$, $r_{101} = t_{101} = 1.0$, thus already scaled from the start as required, and by evaluating the surfaces at the 10201 points identified above in the order as specified above and in the Introduction section in [3], a discretization of each surface was obtained consisting

of 10201 points. Given a pair of surfaces of one of the three kinds mentioned above, discretized as just described, then during the execution of our software package on their discretizations, using software based on both dynamic programming and gradient descent, used separately or combined, one surface was identified as the first surface, the other one as the second surface (in the methods presented in the previous section and in [3], using gradient descent and/or dynamic programming, the second surface is reparametrized while the first one is rotated). For the purpose of testing the capability of the software, again using the same notation used above in this section, given γ, a bijective function on the unit square to be defined below, with $(\hat{r}_i, \hat{t}_j) = \gamma(r_i, t_j),\ i = 1, \ldots, 101,\ j = 1, \ldots, 101$, the second surface was reparametrized through its discretization, namely by setting $\hat{c}_2 = c_2$ and computing $c_2(r_i, t_j) = \hat{c}_2(\hat{r}_i, \hat{t}_j)$, $i = 1, \ldots, 101,\ j = 1, \ldots, 101$, while the first surface was kept as originally defined and discretized by computing $c_1(r_i, t_j)$, $i = 1, \ldots, 101,\ j = 1, \ldots, 101$. All of the above done, the software package then was executed twice, each time using the discretizations of the surfaces as just described in terms of c_1, c_2, etc., to compute an approximation of the area of each surface and scale each surface to have approximate area equal to 1, and then compute an elastic shape registration of the two surfaces and the elastic shape distance between them associated with the registration, the first time using gradient descent with dynamic programming, the second time using gradient descent without dynamic programming. Note, in what follows, numbers obtained as elastic shape distances are actually the square of these distances.

The first results that follow were obtained from applications of our software package on discretizations of surfaces in $3-$dimensional space that are actually graphs of functions based on the sine curve. Given k, a positive integer, one type of surface to which we refer as a surface of the sine kind (type 1) is defined by

$$x(r, t) = r, \quad y(r, t) = t, \quad z(r, t) = \sin k\pi r, \quad (r, t) \in [0, 1] \times [0, 1],$$

and another one (type 2) by

$$x(r, t) = \sin k\pi r, \quad y(r, t) = r, \quad z(r, t) = t, \quad (r, t) \in [0, 1] \times [0, 1],$$

the former a rotation of the latter by applying the rotation matrix $\left(\begin{smallmatrix} 0 & 1 & 0 \\ 0 & 0 & 1 \\ 1 & 0 & 0 \end{smallmatrix}\right)$ on the latter, thus of similar shape.

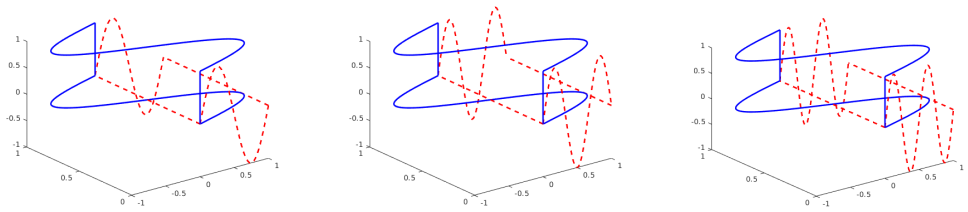


Figure 2: Three plots of boundaries of surfaces of the sine kind. Elastic shape registrations of the two surfaces in each plot were computed using gradient descent, with and without dynamic programming.

Three plots depicting surfaces (actually their boundaries in solid blue and dashed red) of the sine kind for different values of k are shown in Figure 2. (Note that in the plots there, the $x-$, $y-$, $z-$ axes are not always to scale relative to one another). In each plot two surfaces of the sine kind appear. The two surfaces in the leftmost plot being of similar shape, clearly the elastic shape distance between them is exactly zero, and the hope was then that the execution of our software package applied on these two surfaces, using gradient descent and/or dynamic programming, would produce an elastic shape distance between them equal or close to zero. The type 2 surface in each plot (in solid blue) was considered to be the first surface in the plot. In each plot this surface was obtained by setting k equal to 2 in the definition above of a type 2 surface of the sine kind so that it is the same surface in all three plots. The other surface in each plot (in dashed red) is a type 1 surface of the sine kind and was considered to be the second surface in each plot. From left to right in the three plots, the second surface was obtained by setting k equal to 2, 3, 4, respectively, in the definition above of a type 1 surface of the sine kind. As already mentioned above, in the methods presented in the previous section and in [3], using gradient descent and/or dynamic programming, the second surface is reparametrized while the first one is rotated.

With $\gamma(r,t) = (r^{5/4}, t)$, $(r,t) \in [0,1] \times [0,1]$, all surfaces in the plots were discretized as described above and an elastic shape registration of the two surfaces in each plot together with the elastic shape distance between them associated with the registration were computed through executions of our software package, using gradient descent and/or dynamic programming. We

note that for this particular γ, the discretizations of the second surfaces were perturbed only in the r direction which made the software package more likely to succeed just by using dynamic programming, before using gradient descent, as it is perturbations in the r direction that the dynamic programming software is equipped to handle.

Using dynamic programming followed by gradient descent, the results were as follows. The three elastic shape distances computed with dynamic programming before using gradient descent, in the order of the plots from left to right, were as follows with the first distance, as hoped for, essentially equal to zero: 0.00031, 0.3479, 0.3192. The times of execution in the same order were 28.22, 29.23, 39.97 seconds. The computed optimal rotation matrices in the same order were $\begin{pmatrix} -0.0008 & 1 & 0 \\ 0 & 0 & 1 \\ 1 & 0.0008 & 0 \end{pmatrix}$, $\begin{pmatrix} 0.02 & 1 & 0 \\ 0 & 0 & 1 \\ 1 & -0.02 & 0 \end{pmatrix}$, $\begin{pmatrix} 0.03 & 1 & 0 \\ 0 & 0 & 1 \\ 1 & -0.03 & 0 \end{pmatrix}$. The three elastic shape distances computed using gradient descent with the results obtained with dynamic programming used as input, in the order of the plots from left to right, were as follows: 0.00029, 0.3421, 0.3190. The times of execution in the same order were 0.32, 0.44, 0.29 seconds. The computed optimal rotation matrices in the same order were $\begin{pmatrix} 0.00001 & 1 & 0 \\ 0 & 0 & 1 \\ 1 & -0.00001 & 0 \end{pmatrix}$, $\begin{pmatrix} 0.02 & 1 & 0 \\ 0 & 0 & 1 \\ 1 & -0.02 & 0 \end{pmatrix}$, $\begin{pmatrix} 0.03 & 1 & 0 \\ 0 & 0 & 1 \\ 1 & -0.03 & 0 \end{pmatrix}$. Note, perhaps because the discretizations of the second surfaces were perturbed only in the r direction, dynamic programming alone appears to have produced good solutions while gradient descent doesn't appear to have improved these solutions in a significant way. On the other hand, using gradient descent without dynamic programming, i.e., gradient descent with initial solution the identity matrix and the identity diffeomorphism, the results were as follows. The three elastic shape distances in the order of the plots from left to right were 0.25, 1.02, 0.7058. The times of execution in the same order were 3.68, 1.58, 2.36 seconds. The computed optimal rotation matrices in the same order were $\begin{pmatrix} 0.02 & 1 & 0 \\ 0 & 0 & 1 \\ 1 & -0.02 & 0 \end{pmatrix}$, $\begin{pmatrix} -0.02 & 1 & 0 \\ 0 & 0 & 1 \\ 1 & 0.02 & 0 \end{pmatrix}$, $\begin{pmatrix} -0.08 & 1 & 0 \\ 0 & 0 & 1 \\ 1 & 0.08 & 0 \end{pmatrix}$. Clearly these results obtained using gradient descent with initial solution the identity matrix and the identity diffeomorphism are far from optimal.

Finally, with $\gamma(r,t) = (r^{5/4}, t^{5/4})$, $(r,t) \in [0,1]\times[0,1]$, again all surfaces in the plots were discretized as described above and an elastic shape registration of the two surfaces in each plot together with the elastic shape distance between them associated with the registration were computed through executions of our software package, using gradient descent and/or dynamic programming.

We note that for this particular γ, the discretizations of the second surfaces were perturbed in both the r and the t directions which made the dynamic programming software less likely to succeed by itself as it is equipped to handle perturbations in the r direction but not in the t direction.

Using dynamic programming followed by gradient descent, the results were as follows. The three elastic shape distances computed with dynamic programming before using gradient descent, in the order of the plots from left to right, were as follows with the first distance close to zero but not enough: 0.0126, 0.3565, 0.3282. The times of execution in the same order were 28.76, 49.37, 40.75 seconds. The computed optimal rotation matrices in the same order were $\begin{pmatrix} -0.001 & 1 & 0 \\ 0 & 0 & 1 \\ 1 & 0.001 & 0 \end{pmatrix}$, $\begin{pmatrix} 0.02 & 1 & -0.00008 \\ -0.0002 & 0.00009 & 1 \\ 1 & -0.02 & 0.0002 \end{pmatrix}$, $\begin{pmatrix} 0.03 & 1 & 0.0007 \\ 0.002 & -0.0008 & 1 \\ 1 & -0.03 & -0.002 \end{pmatrix}$. The three elastic shape distances computed using gradient descent with the results obtained with dynamic programming used as input, in the order of the plots from left to right, were as follows: 0.00302, 0.3493, 0.3234. The times of execution in the same order were 2.73, 0.77, 0.65 seconds. The computed optimal rotation matrices in the same order were $\begin{pmatrix} -0.0001 & 1 & 0 \\ 0 & 0 & 1 \\ 1 & 0.0001 & 0 \end{pmatrix}$, $\begin{pmatrix} 0.03 & 1 & -0.0003 \\ -0.0007 & 0.0003 & 1 \\ 1 & -0.03 & 0.0007 \end{pmatrix}$, $\begin{pmatrix} 0.03 & 1 & 0.001 \\ 0.005 & -0.002 & 1 \\ 1 & -0.03 & -0.005 \end{pmatrix}$. Note, perhaps because the discretizations of the second surfaces were perturbed in both the r and t directions, and the dynamic programming software is not equipped to handle perturbations in the t direction, the results from dynamic programming alone, although not far from optimal were not exactly optimal. Note as well, gradient descent did improve these results somewhat, the first distance becoming closer to zero. On the other hand, using gradient descent without dynamic programming, i.e., gradient descent with initial solution the identity matrix and the identity diffeomorphism, the results were as follows. The three elastic shape distances in the order of the plots from left to right were 0.32, 0.70, 0.6262. The times of execution in the same order were 4.62, 5.40, 3.67 seconds. The computed optimal rotation matrices in the same order were $\begin{pmatrix} 0.008 & 1 & -0.002 \\ 0.004 & 0.002 & 1 \\ 1 & -0.008 & -0.004 \end{pmatrix}$, $\begin{pmatrix} 0.009 & -1 & -0.002 \\ 0.009 & 0.002 & -1 \\ 1 & 0.009 & 0.009 \end{pmatrix}$, $\begin{pmatrix} 0.001 & -1 & 0.0001 \\ 0.0007 & -0.0001 & -1 \\ 1 & 0.001 & 0.0007 \end{pmatrix}$. Clearly these results obtained using gradient descent with initial solution the identity matrix and the identity diffeomorphism are far from optimal.

The next results that follow were obtained from applications of our software package on discretizations of surfaces in 3−dimensional space of the helicoid kind. Given k, a positive integer, one type of surface to which we refer as a

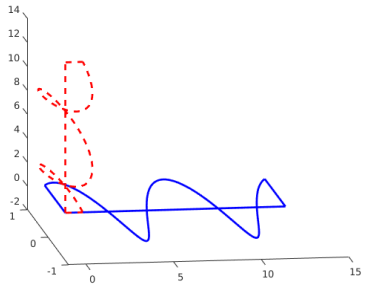


Figure 3: Boundaries of two surfaces of similar shape of the helicoid kind for $k = 4$, type 1 in dashed red, type 2 in solid blue.

surface of the helicoid kind (type 1) is defined by

$$x(r,t) = r\cos k\pi t, \quad y(r,t) = r\sin k\pi t, \quad z(r,t) = k\pi t, \quad (r,t) \in [0,1]\times[0,1],$$

and another one (type 2) by

$$x(r,t) = k\pi t, \quad y(r,t) = r\cos k\pi t, \quad z(r,t) = r\sin k\pi t, \quad (r,t) \in [0,1]\times[0,1],$$

the former a rotation of the latter by applying the rotation matrix $\left(\begin{smallmatrix} 0 & 1 & 0 \\ 0 & 0 & 1 \\ 1 & 0 & 0 \end{smallmatrix}\right)$ on the latter, thus of similar shape.

A plot depicting two surfaces (actually their boundaries) of similar shape of the helicoid kind for $k = 4$ is shown in Figure 3. (Note that in the plot there, the $x-$, $y-$, $z-$ axes are not always to scale relative to one another). The two surfaces being of similar shape, clearly the elastic shape distance between them is exactly zero, and the hope was once again that the execution of our software package applied on these two surfaces, using gradient descent and/or dynamic programming, would produce an elastic shape distance between them equal or close to zero. The type 2 surface of the helicoid kind in the plot (in solid blue) was considered to be the first surface in the plot. The other surface in the plot (in dashed red) is a type 1 surface of the helicoid kind and was considered to be the second surface in the plot.

With $\gamma(r,t) = (r^{5/4}, t)$, $(r,t) \in [0,1]\times[0,1]$, the two surfaces in the plot were discretized as described above and an elastic shape registration of the two surfaces together with the elastic shape distance between them associated

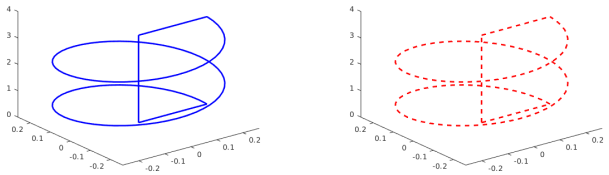


Figure 4: For $\gamma(r,t) = (r^{5/4}, t)$, $(r,t) \in [0,1] \times [0,1]$, after dynamic programming, before gradient descent, views of boundary of rotated first surface (solid blue), and of reparametrized second surface (dashed red).

with the registration were computed through the execution of our software package, using gradient descent and/or dynamic programming. Again we note that for this particular γ, the discretization of the second surface was perturbed only in the r direction which as pointed out above made the software package more likely to succeed just by using dynamic programming, before using gradient descent.

Using dynamic programming followed by gradient descent, the results were as follows. The elastic shape distance computed with dynamic programming before using gradient descent was 0.00019, which, as hoped for, was close enough to zero. The time of execution was 15.32 seconds. The computed optimal rotation matrix was $\begin{pmatrix} 0 & 1 & 0 \\ 0 & 0 & 1 \\ 1 & 0 & 0 \end{pmatrix}$. Views of the two surfaces after dynamic programming, before gradient descent, are shown in Figure 4. The elastic shape distance computed using gradient descent with the results obtained with dynamic programming used as input was 0.00018. The time of execution was 0.23 seconds. The computed optimal rotation matrix was $\begin{pmatrix} 0 & 1 & 0 \\ 0 & 0 & 1 \\ 1 & 0 & 0 \end{pmatrix}$. Note, perhaps because the discretization of the second surface was perturbed only in the r direction, dynamic programming alone appears to have produced good solutions while gradient descent doesn't appear to have improved these solutions in a significant way. On the other hand, using gradient descent without dynamic programming, i.e., gradient descent with initial solution the identity matrix and the identity diffeomorphism, the results were as follows. The elastic shape distance was 0.11. The time of execution was 13.42 seconds. The computed optimal rotation matrix was $\begin{pmatrix} 0.01 & 1 & -0.06 \\ -0.02 & 0.06 & 1 \\ 1 & -0.01 & 0.02 \end{pmatrix}$. Clearly these results obtained using gradient descent with initial solution the identity ma-

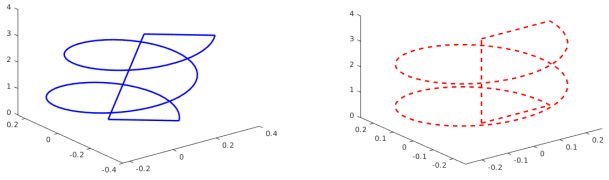


Figure 5: For $\gamma(r,t) = (r^{5/4}, t^{5/4})$, $(r,t) \in [0,1] \times [0,1]$, after dynamic programming, before gradient descent, views of boundary of rotated first surface (solid blue), and of reparametrized second surface (dashed red).

trix and the identity diffeomorphism, although not necessarily bad, are still far from optimal.

Finally, with $\gamma(r,t) = (r^{5/4}, t^{5/4})$, $(r,t) \in [0,1] \times [0,1]$, again the two surfaces in the plot were discretized as described above and an elastic shape registration of the two surfaces together with the elastic shape distance betwen them associated with the registration were computed through the execution of our software package, using gradient descent and/or dynamic programming. Again we note that for this particular γ, the discretization of the second surface was perturbed in both the r and the t directions which as pointed out above made the dynamic programming software less likely to succeed by itself as it is equipped to handle perturbations in the r direction but not in the t direction.

Using dynamic programming followed by gradient descent, the results were as follows. The elastic shape distance computed with dynamic programming before using gradient descent was 0.0796 which was not far from zero but not close enough. The time of execution was 19.59 seconds. The computed optimal rotation matrix was $\begin{pmatrix} 0.03 & 0.8 & 0.7 \\ -0.03 & -0.7 & 0.8 \\ 1 & -0.04 & 0.004 \end{pmatrix}$. Views of the two surfaces after dynamic programming, before gradient descent, are shown in Figure 5. The elastic shape distance computed using gradient descent with the results obtained with dynamic programming used as input was 0.00876. The time of execution was 6.70 seconds. The computed optimal rotation matrix was $\begin{pmatrix} 0.01 & 1 & 0.07 \\ -0.004 & -0.07 & 1 \\ 1 & -0.01 & 0.003 \end{pmatrix}$. Views of the two surfaces after dynamic programming followed by gradient descent are shown in Figure 6. Note, perhaps because

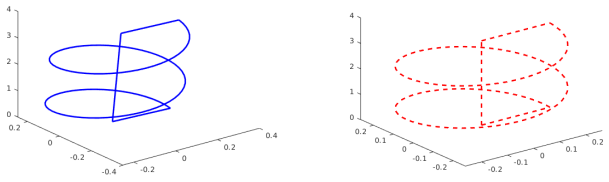


Figure 6: For $\gamma(r,t) = (r^{5/4}, t^{5/4})$, $(r,t) \in [0,1] \times [0,1]$, after dynamic programming followed by gradient descent, views of boundary of rotated first surface (solid blue), and of reparametrized second surface (dashed red).

the discretization of the second surface was perturbed in both the r and t directions, and the dynamic programming software is not equipped to handle perturbations in the t direction, the results from dynamic programming alone, although not far from optimal were not exactly optimal. Note as well, gradient descent did improve these results somewhat, the distance becoming closer to zero. On the other hand, using gradient descent without dynamic programming, i.e., gradient descent with initial solution the identity matrix and the identity diffeomorphism, the results were as follows. The elastic shape distance was 0.0943. The time of execution was 15.80 seconds. The computed optimal rotation matrix was $\begin{pmatrix} 0.01 & 1 & -0.05 \\ -0.02 & 0.05 & 1 \\ 1 & -0.01 & 0.02 \end{pmatrix}$. Clearly these results obtained using gradient descent with initial solution the identity matrix and the identity diffeomorphism, although not necessarily bad, are still far from optimal.

The final results that follow were obtained from applications of our software package on discretizations of two surfaces in $3-$dimensional space that are actually graphs of functions based on the product of the cosine and sine functions. One surface to which we refer as the type 1 surface of the cosine-sine kind is defined by

$$x(r,t) = r, \quad y(r,t) = t, \quad z(r,t) = (\cos 0.5\pi r)(\sin 0.5\pi t), \quad (r,t) \in [0,1] \times [0,1],$$

and the other surface to which we refer as the type 2 surface of the cosine-sine kind is defined by

$$x(r,t) = (\cos 0.5\pi r)(\sin 0.5\pi t), \quad y(r,t) = r, \quad z(r,t) = t, \quad (r,t) \in [0,1] \times [0,1],$$

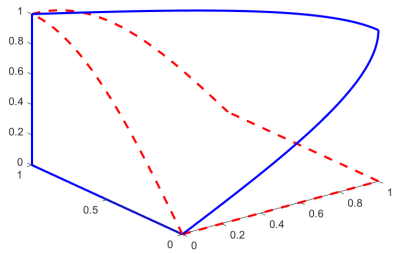


Figure 7: Boundaries of the two surfaces of the cosine-sine kind, the type 1 surface in dashed red, the type 2 surface in solid blue.

the former a rotation of the latter by applying the rotation matrix $\begin{pmatrix} 0 & 1 & 0 \\ 0 & 0 & 1 \\ 1 & 0 & 0 \end{pmatrix}$ on the latter, thus of similar shape.

A plot depicting the two surfaces (actually their boundaries) of the cosine-sine kind is shown in Figure 7. (Note that in the plot there, the $x-$, $y-$, $z-$ axes are not always to scale relative to one another). The two surfaces being of similar shape, clearly the elastic shape distance between them is exactly zero, and the hope was once again that the execution of our software package applied on these two surfaces would produce an elastic shape distance between them equal or close to zero. The type 2 surface of the cosine-sine kind in the plot (in solid blue) was considered to be the first surface in the plot. The other surface in the plot (in dashed red) is the type 1 surface of the cosine-sine kind and was considered to be the second surface in the plot.

With $\gamma(r,t) = (r^{5/4}, t)$, $(r,t) \in [0,1] \times [0,1]$, the two surfaces in the plot were then discretized as described above and an elastic shape registration of the two surfaces and the elastic shape distance between them associated with the registration were then computed through the execution of our software package, using gradient descent and/or dynamic programming. Again we note that for this particular γ, the discretization of the second surface was perturbed only in the r direction which as pointed out above made the software package more likely to succeed just by using dynamic programming before using gradient descent.

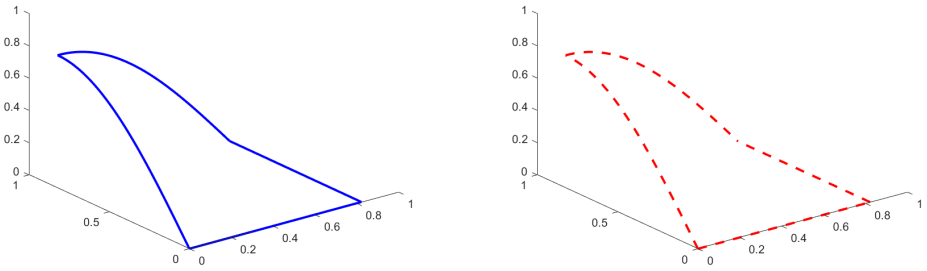


Figure 8: For $\gamma(r,t) = (r^{5/4}, t)$, $(r,t) \in [0,1] \times [0,1]$, after dynamic programming, before gradient descent, views of boundary of rotated first surface (solid blue), and of reparametrized second surface (dashed red).

Using dynamic programming followed by gradient descent, the results were as follows. The elastic shape distance computed with dynamic programming before using gradient descent was 0.00021, which, as hoped for, was close enough to zero. The time of execution was 22.29 seconds. The computed optimal rotation matrix was $\begin{pmatrix} -0.001 & 1 & 0.0009 \\ -0.001 & -0.0009 & 1 \\ 1 & 0.001 & 0.001 \end{pmatrix}$. Views of the two surfaces after dynamic programming, before gradient descent, are shown in Figure 8. The elastic shape distance computed using gradient descent with the results obtained with dynamic programming used as input was 0.00019. The time of execution was 0.23 seconds. The computed optimal rotation matrix was $\begin{pmatrix} -0.0006 & 1 & 0.0004 \\ -0.0005 & -0.0004 & 1 \\ 1 & 0.0006 & 0.0005 \end{pmatrix}$. Note, perhaps because the discretization of the second surface was perturbed only in the r direction, dynamic programming alone appears to have produced good solutions while gradient descent doesn't appear to have improved these solutions in a significant way. On the other hand, using gradient descent without dynamic programming, i.e., gradient descent with initial solution the identity matrix and the identity diffeomorphism, the results were as follows. The elastic shape distance was 0.47. The time of execution was 3.12 seconds. The computed optimal rotation matrix was $\begin{pmatrix} 0.03 & 1 & -0.1 \\ -0.07 & 0.1 & 1 \\ 1 & -0.02 & 0.07 \end{pmatrix}$. Clearly these results obtained using gradient descent with initial solution the identity matrix and the identity diffeomorphism are far from optimal.

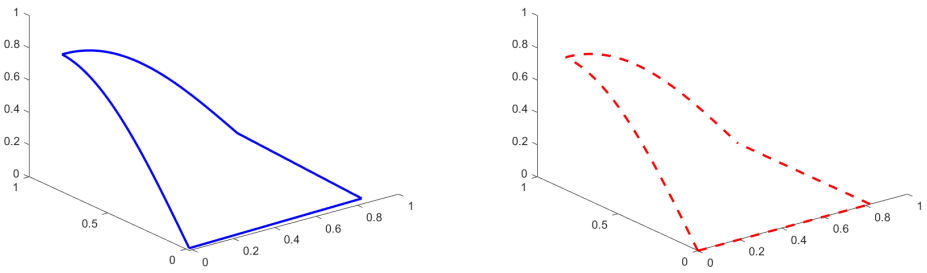


Figure 9: For $\gamma(r,t) = (r^{5/4}, t^{5/4})$, $(r,t) \in [0,1] \times [0,1]$, after dynamic programming, before gradient descent, views of boundary of rotated first surface (solid blue), and of reparametrized second surface (dashed red).

Finally, with $\gamma(r,t) = (r^{5/4}, t^{5/4})$, $(r,t) \in [0,1] \times [0,1]$, again the two surfaces in the plot were discretized as described above and an elastic shape registration of the two surfaces together with the elastic shape distance betwen them associated with the registration were computed through the execution of our software package, using gradient descent and/or dynamic programming. Again we note that for this particular γ, the discretization of the second surface was perturbed in both the r and the t directions which as pointed out above made the dynamic programming software less likely to succeed by itself as it is equipped to handle perturbations in the r direction but not in the t direction.

Using dynamic programming followed by gradient descent, the results were as follows. The elastic shape distance computed with dynamic programming before using gradient descent was 0.0143 which was not far from zero but not close enough. The time of execution was 23.54 seconds. The computed optimal rotation matrix was $\begin{pmatrix} -0.04 & 1 & 0.03 \\ -0.04 & -0.03 & 1 \\ 1 & 0.04 & 0.04 \end{pmatrix}$. Views of the two surfaces after dynamic programming, before gradient descent, are shown in Figure 9. The elastic shape distance computed using gradient descent with the results obtained with dynamic programming used as input was 0.0033. The time of execution was 2.11 seconds. The computed optimal rotation matrix was $\begin{pmatrix} -0.02 & 1 & 0.008 \\ -0.02 & -0.008 & 1 \\ 1 & 0.02 & 0.02 \end{pmatrix}$. Views of the two surfaces after dynamic programming followed by gradient descent are shown in Figure 10. Note, perhaps because

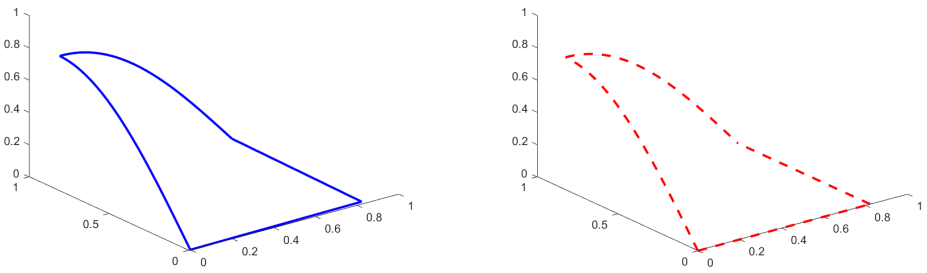


Figure 10: For $\gamma(r,t) = (r^{5/4}, t^{5/4})$, $(r,t) \in [0,1] \times [0,1]$, after dynamic programming followed by gradient descent, views of boundary of rotated first surface (solid blue), and of reparametrized second surface (dashed red).

the discretization of the second surface was perturbed in both the r and t directions, and the dynamic programming software is not equipped to handle perturbations in the t direction, the results from dynamic programming alone, although not far from optimal were not exactly optimal. Note as well, gradient descent did improve these results somewhat, the distance becoming closer to zero. On the other hand, using gradient descent without dynamic programming, i.e., gradient descent with initial solution the identity matrix and the identity diffeomorphism, the results were as follows. The elastic shape distance was 0.4791. The time of execution was 3.28 seconds. The computed optimal rotation matrix was $\begin{pmatrix} 0.01 & 1 & -0.1 \\ -0.08 & 0.1 & 1 \\ 1 & -0.003 & 0.08 \end{pmatrix}$. Clearly these results obtained using gradient descent with initial solution the identity matrix and the identity diffeomorphism are far from optimal.

Summary

In this paper we have presented results from computing the elastic shape registration of two simple surfaces in 3−dimensional space and the elastic shape distance between them with an algorithm based on a gradient descent approach for reparametrizing one of the surfaces, using as the input initial solution to the algorithm the rotation and reparametrization computed with the algorithm based on dynamic programming presented in [3] for reparametrizing one of the surfaces to obtain a partial elastic shape reg-

istration of the surfaces. The gradient descent approach used to obtain our results is a generalization to surfaces in 3−dimensional space of the gradient descent approach for reparametrizing one of two curves in the plane when computing the elastic shape distance between them as presented in [13]. We have described and justified the approach for curves as it is done in [13], and have presented and justified its generalization to surfaces in 3−dimensional space. Our algorithm based on gradient descent and dynamic programming as just described has been implemented in the form of a software package written in Matlab with the exception of the dynamic programming routine which is written in Fortran but executed as a Matlab mex file. The results we have presented in this paper were obtained from applications of the software package on discretizations of the three kinds of surfaces in 3−dimensional space identified in [3] as surfaces of the sine, helicoid and cosine-sine kind. Some of these results verify that dynamic programming alone as implemented produces good results essentially optimal for surfaces whose parametrizations have been perturbed only in the $x-$direction of the plane as it is perturbations in this direction that dynamic programming as implemented is equipped to handle. On the other hand, other results verify that dynamic programming alone as implemented produces results not far from optimal but still not optimal for surfaces whose parametrizations have been perturbed in the $y-$direction of the plane as well. For this situation, other results show that gradient descent using as input the results obtained with dynamic programming produces results closer to optimal than dynamic programming alone as implemented. However some results show that gradient descent alone without dynamic programming, i.e., gradient descent with initial solution the identity matrix and the identity diffeomorphism produces results far from optimal almost every time.

References

[1] Bernal, J.: Shape Analysis, Lebesgue Integration and Absolute Continuity Connections. NISTIR 8217 (2018).

[2] Bernal, J., Lawrence, J., Dogan, G., Hagwood, C. R.: On Computing Elastic Shape Distances between Curves in d-dimensional Space. NIST Technical Note 2164 (2021)

[3] Bernal, J., Lawrence, J.: Partial Elastic Shape Registration of 3D Surfaces using Dynamic Programming. NIST Technical Note 2274 (2023)

[4] Dogan, G., Bernal, J., Hagwood, C. R.: FFT-based alignment of 2d closed curves with application to elastic shape analysis. Proceedings of the 1st DIFF-CV Workshop, British Machine Vision Conference, Swansea, Wales, UK. September 2015.

[5] Gale, D., Nikaido, H.: The Jacobian matrix and global univalence of mappings. Math. Annalen. 159: 81-93 (1965).

[6] Jermyn, I. H., Kurtek, S., Klassen, E., and Srivastava, A.: Elastic shape matching of parameterized surfaces using square root normal fields. Proceedings of the 12th European Conference on Computer Vision (ECCV'12), Volume V, pp. 804-–817. Springer, Berlin (2012)

[7] Joshi, S. H., Klassen, E., Srivastava, A., and Jermyn, I. H.: A novel representation for riemannian analysis of elastic curves in R^n. Proceedings of the IEEE Conference on Computer Vision and Pattern Recognition (CVPR), Minneapolis, MN. June 2007.

[8] Kabsch, W.: A solution for the best rotation to relate two sets of vectors. Acta Crystallographica Section A: Crystal Physics. 32(5): 922-923 (1976).

[9] Kabsch, W.: A discussion of the solution for the best rotation to relate two sets of vectors. Acta Crystallographica Section A: Crystal Physics. 34(5): 827-828 (1978).

[10] Kurtek, S., Klassen, E., Ding, Z., Srivastava, A.: A novel riemannian framework for shape analysis of 3D objects. Proceedings of the IEEE Conference on Computer Vision and Pattern Recognition (CVPR), San Francisco, CA. June 2010.

[11] Lawrence, J., Bernal, J., Witzgall, C.: A Purely Algebraic Justification of the Kabsch-Umeyama Algorithm. Journal of Research of the National Institute of Standards and Technology. 124 (2019).

[12] Riseth, J. N.: Gradient Based Algorithms in Shape Analysis for Reparametrization of Parametric Curves and Surfaces. Master's thesis in Applied Physics and Mathematics, Norwegian University of Science

and Technology, Faculty of Information Technology and Electrical Engineering, Department of Mathematical Sciences, February 2021.

[13] Srivastava, A., Klassen, E. P.: Functional and Shape Data Analysis. New York: Springer. (2016)

[14] Srivastava, A., Klassen, E. P., Joshi, S. H., Jermyn, I. H.: Shape Analysis of Elastic Curves in Euclidean Spaces. IEEE Trans. Pattern Analysis and Machine Intelligence. 33(7): 1415-1428 (2011).

[15] Umeyama, S.: Least-Squares Estimation of Transformation Parameters Between Two Point Patterns. IEEE Trans. Pattern Analysis and Machine Intelligence. 13(4): 376-380 (1991).